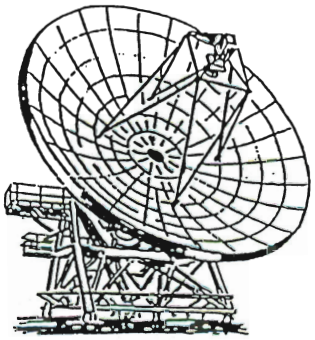

The JCMT - UKIRT NEWSLETTER

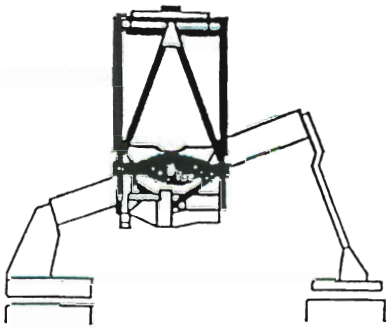

Kūlia I Ka Nu'U

Number 4 August 1992

Jupiter from pole to pole

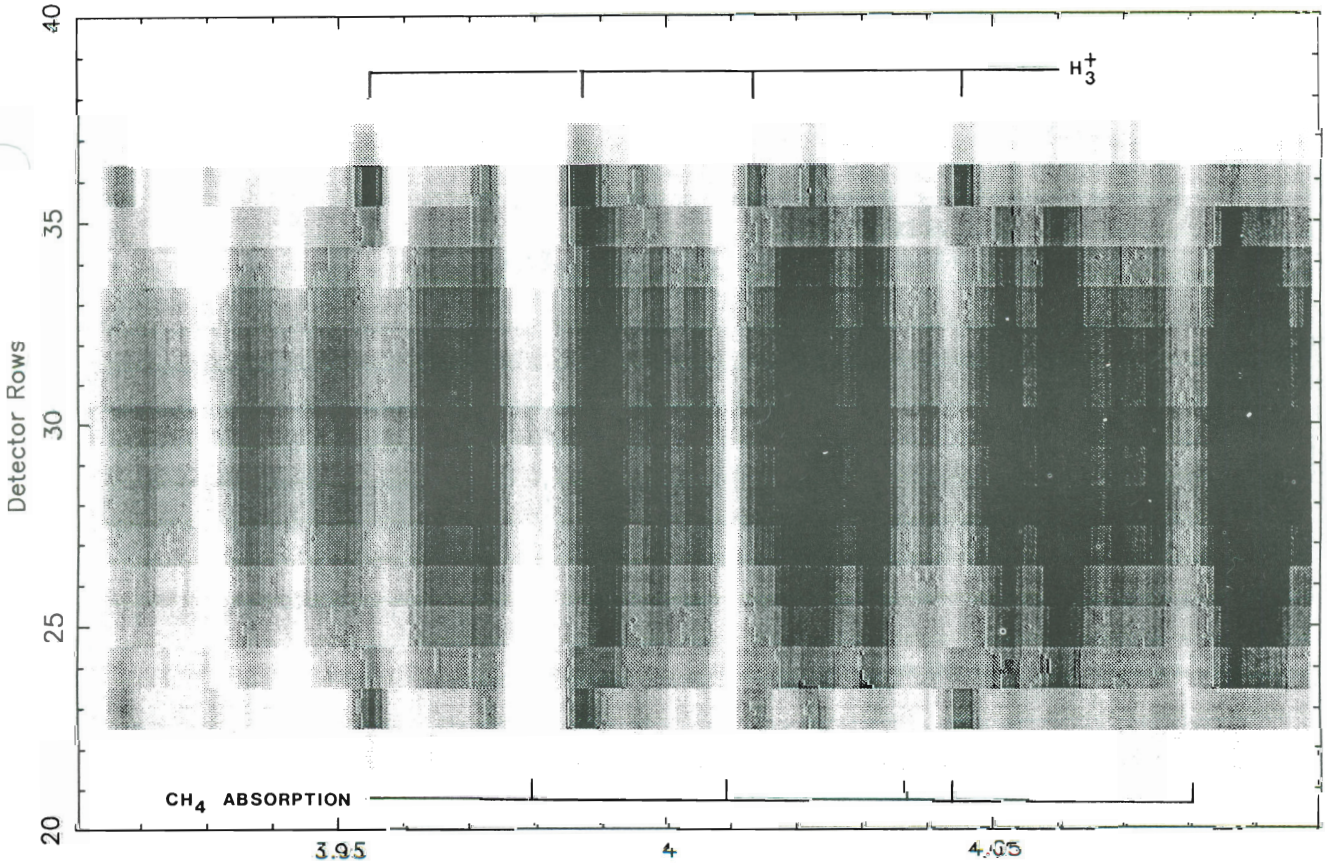

Wavelength in Microns

Contents

Cover Picture:

H_3^+ Emission from the Poles of Jupiter

Spectral image of Jupiter from 3.9 to 4.1 microns, obtained by S. Miller, L. Trafton, and T. Geballe with CGS4 on April 2, 1992, using a pixel scale of 3.07 arcseconds/pixel. The CGS4 slit was orientated along the polar axis of Jupiter; North is up. The spectra of central regions of the planet contain a bright continuum and strong methane absorptions. At the poles several H3+ lines can be seen in emission, superimposed on a weaker continuum and methane absorption spectrum. The brightest H3+ lines are approximately at 3.95, 3.99, and 4.04 microns, and are members of the Q-branch of the v2 fundamental vibration-rotation band. The spectrum was obtained in approximately ten minutes of integration time.

People

Yolanda Boyce left the JAC in March after many years as a UKIRT Secretary before becoming a JAC Secretary after the commissioning of the JCMT.

Dayna Oda-Kell has joined the Secretarial Section. Dayna comes with lots of experience from the travel industry. A native of the Big Island, Dayna is a professional entertainer and won the title of Miss Aloha Hula at the Merry Monarch competition in 1982.

Mark Casali left the JAC in March to return to ROE. Mark had maintained overall responsibility for IRCAM for the past few years.

Matt Mountain arrived at the JAC in January to begin a tour of duty from ROE. Matt is the Project Scientist for CGS4. At this time, however, Matt is poised to leave the JAC to take up the position of International GEMINI Project Scientist in Tucson.

Roger Carvalho left the JAC in April to join the local Fire Department. Roger was an Electronic Technician with the JAC for several years.

Graeme Watt left the JAC in April to return to ROE. Graeme had been Operations Manager for the JCMT since the beginning. He now joins the Edinburgh operations group.

Liz Sim, the first editor of this joint newsletter, has taken early retirement after 26 years at ROE. Liz will not be "retired" for long, however, as she plans to fulfill a long-held ambition to study theology.

Margaret Johnston left the JAC at the end of April to return to RAL. Margaret had been the Administration Officer at the JAC for the past 4 years.

Ian Midson has joined the JAC as Administration Officer starting in May. Ian was formerly Executive Secretary for the PATT at the SERC, Swindon.

Chris Purton has joined the JAC to take over the challenging job of Operations Manager for the JCMT. Chris will be looking after the schedule, chairing scheduling meetings and generally keeping observers on the straight and narrow. He arrives from Penticton in British Columbia as another Canadian member of staff.

Gary Dalton has been employed by the JAC on a 6-month term to assist Simon Craig as a Mechanical Engineer. Gary will be working on the redesign of the JCMT roof side-thrust roller unit, SCUBA, the UPS/SPS cover and the AZ track brackets.

Ian Robson has been appointed by the JCMT Board as the new Director JCMT. It is likely that Ian will take up his post around December.

Richard Wade has been appointed as Head of the Applied Physics Division at RAL. Richard will be leaving his post as Acting Director, JCMT and returning to the UK towards the end of the year.

Address Change

Please note that with immediate effect the Joint Astronomy Centre has a new address:

660 N. A'Ohoku Place,
University Park,
Hilo, HI 96720
U.S.A.

The post office will continue to redirect mail addressed to 665 Komohana Street for some time.

As a result of the construction of the new entrance to the Science Park, the old Komohana Street entrance to the JAC is no longer open. All traffic must now enter the Park through the new opening on Komohana Street.

New Management

You may notice that there is a new selection of editors for this Newsletter. Thereupon you may find a few changes in content and format once we get our act together. Please send any comments, ideas, criticisms, etc. to the ROE team of Eve, Mark and Graeme, or Colin Aspin at JAC. Remember, this is YOUR Newsletter — we just put it together in a presentable fashion!

Remote Observing with either the JCMT or with the UKIRT

Remote observing is available with both telescopes, from any suitable site in the UK. For the JCMT remote observing is also available from Canada and the Netherlands. All JCMT instruments should be usable. All UKIRT instruments except CGS4 may be used. The manual "Remote Observing with JCMT and UKIRT" is available on request.

The remote observing system is very easy to use. A remote observer (RO) logs on to one of the remote-observing usernames at the telescope and selects from a menu which of the observing screens he/she wants to see. Usually the RO has a separate login for each screen, although it is also possible to swap between screens from a single login. There are mechanisms for file transfers and for communications with people at the telescope.

There are two possibilities for remote observing with UKIRT: passive observing and active observing. With passive observing the RO watches progress at the telescope but does not control any of the observations. However, with active observing the RO can watch progress and control the observations. Authorisation is needed for both passive and active observing, and active observing will be more restricted.

At the JCMT it is routine procedure for the telescope operator to control the observations, and so passive observing is appropriate and efficient. However, active observing, in which the RO can also control the observations, is available on request.

ROE has a quiet remote-observing room, well equipped with: a colour-graphics VAXstation 3100 (DECwindows Motif); a colour-graphics VAXstation 2000 (DECwindows Motif); two Pericom MG100 terminals (i.e. VT/Tek-type); plenty of disk space, manuals for remote observing, instruments and software; The Astronomical Almanac; a fax machine; telephones; desk space etc. Usually people who are using the remote observing system for the first time travel to ROE so that they can be introduced to the remote observing system and have support staff available. Those who have used the system before often like to return to ROE because of these dedicated facilities in the remote-observing room, the support staff, and the absence of normal disturbances. However, remote observing using the RO's local computer facilities is also becoming quite common now.

The 56 kbit/sec dedicated line from ROE to JACH and the telescopes is available for remote observing and general network connections not just from ROE but from Starlink and Janet nodes throughout the UK. The line is continuing to be very reliable. If you are planning to use your local computer facilities for remote observing then be sure to check that your connection to the dedicated line will not be affected by any maintenance of JANET on Tuesday mornings. ROs in Canada and the Netherlands will use their Internet links.

The two compressed voice channels, multiplexed onto the dedicated line, were available briefly but then withdrawn because of induced unreliability of network connections and other problems. We hope that these problems will be solved soon.

Observers are encouraged to participate in remote observing. At this stage however it is still expected that one member of the JCMT observing team will travel to Hawaii. Note that remote observing allows participation by collaborators now that SERC travel funding is restricted to one observer only in most cases. Also, PATT is identifying UKIRT projects that can be conducted with ROs only and a support scientist at the telescope.

Potential remote observers should contact me for further details. They should also contact their assigned support scientist (and also for UKIRT the astronomer-in-charge) for discussions about feasibility and for authorisation.

Roger Clowes
Royal Observatory
Blackford Hill, Edinburgh

Starlink: REVAD::RGC
Janet: RGC@UK.AC.ROE.STARLINK
SPAN: REVAD::RGC or 19889::RGC
Internet: RGC@STARLINK.ROE.AC.UK

UKIRT News

Expected Availability of UKIRT Instruments during Semester X (February 93 - July 93)

UKT6 single channel 1-5μm photometer, 2.3-4.6μm CVF

UKT8 single channel L', N, Q and narrow band 10μm photometer

UKT9 single channel 1-5μm photometer, 1.35-2.6 μm CVF

UKT16 8-banger; N, Q, 30μm and narrow band 10μm

IRCAM 58x62 array, JHK filters and various narrow band filters in from 1.0 to 4.05μm; 0.6" per pixel (36" field of view), 1.2" (72"); 0.3" per pixel available using ambient temperature 2X magnifier. It is possible that a 256 x 256 array (0.3" pixels, 72" field of view) will be available before the end of Semester X, but this should not be assumed by applicants.

Coronagraph A coronagraph for use with IRCAM is available, subject to the agreement of, and collaboration with, Dr Ben Zuckerman of UCLA, its owner. Applicants should discuss any proposals with Dr Zuckerman before submission of the application.

CGS3 8-22μm grating spectrometer, 1x32 channels, resolving powers of ~60 or 200 at 10μm and ~75 at 20μm, 10μm spectropolarimetry. Beam sizes from 1" to 9" diameter. CGS3 must be mounted on the north or south port, and thus requires that either IRCAM or CGS4 is off the telescope.

CGS4 1-5μm grating and 2D array spectrometer (3" and 1.5" pixel sizes, 75 1/mm, and echelle gratings, ~90" slit, polarizer available. See special CGS4 notes below.

VISPHOT single channel visible B or V photometer, can be operated simultaneously with any of the above single channel instruments.

10 Micron Camera: Berkcam (10 μm camera, 10 or 20 x 64 0.39" pixels, 10% and 1.3% CVFs). The Berkeley group led by J.T. Arens invite UKIRT users to contact them if they wish to make collaborative proposals to use their 10 micron camera on UKIRT in Semester W. Those interested should discuss any potential proposals with the Berkeley group and obtain their agreement to the collaboration prior to submission of the application to PATT. Enquiries should be directed to Dr Chris Skinner, SPAN address: 6913::"skinner@tristan.llnl.gov", INTERNET address: CBS%NSFNET-RELAY::GOV.LLNL.TRISTAN::skinner

IRPOL (1-5μm polarimeter for IRCAM, UKT6, UKT9, CGS3, and CGS4). Note that the unvignetted field of view of IRCAM through IRPOL is ~35"; hence optimal usage of IRCAM+IRPOL is with 0.6" pixels. Commissioning of CGS4+IRPOL and first PATT programs using it are scheduled for Semester W and it is expected that shared risk programs will be viable in Semester X.

FABRY PEROT's - 2μm: 12, 25, 90 and 300 km/s resolutions; can be used with IRCAM, and UKT9; unvignetted field of view through IRCAM is ~ 60" diameter.

Special Notes:

CGS4: Due to the many combinations of gratings and camera focal lengths in CGS4, and the need to minimize the number of changeovers, which require considerable effort and three weeks of down time, some configurations may be avoided during certain semesters, while others may be scheduled during limited periods (at some inconvenience to some observers). It is expected that the CGS4 configurations to be used during Semester X will be advertised to the community one month before the proposal deadline. If more than one CGS4 configuration is acceptable to the applicant, he/she should indicate this on the proposal.

UKT10 (2-banger): At the April meeting of the UPC it was proposed and agreed that this instrument be decommissioned. No observing time has been awarded to it for over two years and it is somewhat redundant with UKT6 and UKT9.

Tom Geballe
Associate Director UKIRT

CGS4 Update

The past year of shared-risks use of the cooled grating spectrometer CGS4 has been an exciting one at UKIRT as user after user has reported new and interesting results from their observing runs. It makes a big difference too, to have an instrument that's capable of observing through even quite thick cirrus. It has been a very busy and productive period as we have developed observing techniques and acquired the ability to handle high data rates, as well as scheduling "down periods" for changing configurations.

150 1/mm Grating Commissioning

The 150 1/mm grating was installed in CGS4 in February for commissioning and use in March-June. The throughput is slightly better than with the 75 1/mm grating, and the lower background and better resolution of OH sky lines is helpful for many programmes. Also the grating efficiency at 2.1 μm in first order is almost twice that expected from the manufacturers' graphs, about 35% instead of 20%, so a wider range of resolutions could be used in the K-window. Users should be aware that the current choice of blocking filters in CGS4 is not ideal for observing around 2.1 μm in second order with this grating. This is the same grating angle as 1.413 μm in 3rd order and 4.24 μm in 1st order. Unfortunately, one of the two potential blocking filters cuts on by 1.4 μm and the other is only just cutting off at 4.2 μm. We will of course attempt to find a better filter, but in the meanwhile — beware.

Long Camera Installation and Commissioning

The successful fitting and installation of the 300 mm camera in CGS4 in Hilo in February was the last major laboratory work in the spectrometer's development, until the installation of the 256 x 256 arrays. The 300mm camera provides twice the resolving power for a given grating, halves the wavelength coverage and halves the pixel scale to 1.5 arcsec e.g. providing a resolution of about 17 km/s with the echelle. Spectra of the galactic centre region are some of the first observations using the long camera. They are also one of the first efficient maps made by automatically stepping the CGS4 slit across a large area, with a record of 512 separate observations being made in one night. These data will be presented in a future issue of the Newsletter.

Commissioning, assessment and documentation of the performance of the long camera is still in progress. The slit length of 90 arcsec illuminates all except one row of the detector with 1.55 arcsec per pixel when the 75 1/mm grating is used. For the echelle anamorphic magnification results in slit and pixel widths about 30% smaller and pixels correspondingly longer with typically about 40 rows illuminated. Both one pixel and two pixel wide slits are available for the echelle and 75 1/mm grating. The wider slits should help when observing in high winds. Using 1.5 arcsec slits is pushing the performance of UKIRT's tracking and guiding capabilities to the limit. The improvements expected as the telescope upgrades programme progresses are going to be greatly appreciated! For best results guide stars are needed and it is well worth allowing time for the TOs to tune the autoguider setup and focus on the IR signal. Finally, if you are relying on blind pointing to find IR faint, optically invisible sources, coordinates accurate to about 0.2 arcsec are needed.

Software Improvements

A speed up of the "movie" display by about a factor 10 and the addition of plots showing vertical and horizontal cuts through the images has resulted in greatly improved efficiency of peaking up. The speed of centering the source in the slit is now limited by the telescope and autoguider settling times rather than the CGS4 movie display.

On the data reduction side several improved features have been added which we quickly found were highly desirable for on-line data assessment. Examples are the ability to fit and remove residual sky lines, and to control easily which flats etc. are used for the reduction. It is hoped to have a version of the data reduction ready for release to Starlink by the end of the year.

A lot of work has also gone into automatically ensuring the safety of data. Raw data are now copied to Hilo within a few seconds of being taken. At the end of the night they are backed up to tape at the summit and any reduced data is copied to Hilo. Raw data and reduced groups are then backed up to optical disk. Once it has been safely backed up, data is automatically deleted from the summit disks if it is more than about 4 days old to ensure space for subsequent nights' observing. In Hilo you can expect your data to be available on disk for up to two weeks, where it is available for you to do further reduction or to write to tape to take away with you. **NB** — if you must leave Hilo immediately after getting down the mountain, please

make arrangements for your support scientist to send a tape to you.

Future Plans

Other modes of CGS4 use which it is hoped to commission this year include spectro-polarimetry and remote observing from the UK. Software work is now in progress to more fully automate peaking up and thereby improve observing efficiency. A Vax-station 4000 model 60 will soon be installed at the summit to replace the existing data reduction work-station. The resulting increase in speed will enable the CGS4 data reduction to keep up with the data acquisition when reducing observations of bright sources.

The short (150mm) focal length camera will be re-installed in CGS4 in October for observing with the echelle and 75 1/mm gratings for at least the remainder of Semester W. We will advertise the CGS4 configurations (camera, gratings) to be used during Semester X to the community one month before the PATT deadline. Some careful scheduling around the ALICE/IRCAM-3 engineering and commissioning work is going to be necessary. The next major development for CGS4 will be the installation of a 256 x 256 array sometime after the IRCAM commissioning.

Gillian Wright
Joint Astronomy Centre
Hilo

Interferometric Measurement of UKIRT Wavefront Errors

Shearing interferometric measurements made with UKIRT last October at folded prime focus and at Cassegrain were highly revealing and produced a sky-mapped description of the third order aberrations of the telescope. By performing the measurements at each of the two focal stations in turn, this allowed separation of effects due to the primary and secondary mirrors.

The equipment used was the ROE Applied Physics parallel plate shearing interferometer together with image intensifier and asynchronous CCD camera. The first results at folded prime focus showed immediately the wavefront distortion due to thermals from the primary mirror cell, producing localised areas of extremely low fringe contrast both by pluming through the central hole of the primary and by convection around the lower edge of the mirror cell when pointing away from zenith. From then on it was necessary to reduce the value of radial shear being used from 4% to 1% to preserve measurable fringes but with the consequence of lowering the measurement accuracy.

The telescope aberrations can be summarised by stating (a) that spherical aberration at the F/36 Cassegrain focus is almost negligible for all pointing directions (wavefront error 0.06 λ peak-to-valley ± 0.2 λ RMS over the sky), (b) that the surface of the primary is close to that of a paraboloid, with conic constant K = -1.0012, (c) that astigmatism is the dominant aberration, giving a wavefront error contribution at the Cassegrain focus of 6 ± 3 λ peak-to-valley depending on sky position for the best of the two orientations investigated of the secondary mirror, and (d) that astigmatism due to the primary mirror contributes peak-to-valley wavefront deformations ranging from 1 λ at small zenith distances to ~ 6 λ at large zenith distances. All of the wavefront measurements were obtained at wavelength λ = 546nm so that at IR wavelengths the values quoted above are reduced with inverse proportionality.

Fortunately, astigmatism in the primary should be relatively easy to correct so this augurs well for image improvements in the UKIRT upgrades programme.

One unexpected finding was the consistent observation of a bright halo around the interferograms obtained at Cassegrain focus, and this remains unexplained. That the halo was not observed at folded prime focus means that the primary mirror and the interferometric equipment itself can be ruled out as the cause.

A report giving the detailed results is obtainable from ROE.

Colin Humphries, ROE
Eli Atad, ROE
Tim Hawarden, JAC

Berkeley Ten Micron Camera available on UKIRT

The UK Berkeley group led by Eric Arens invite UKIRT users to contact them if they wish to make collaborative proposals to use their 10 micron camera on UKIRT in Semester X.

The Berkeley camera currently has 10 x 64 0.39 arcsec pixels giving a field of view of 3.9 x 25 arcsec (N-S x E-W). For mapping extended sources mosaicing is necessary. A sensitivity of 10 mJy/square arcsec/sqrt (minute) has been achieved on UKIRT using a complete N band filter and 20 mJy/square arcsec/sqrt (minute) with a 10% CVF. The camera contains both 10% and 1.3% CVFs for the 10 micron region.

The camera is described by Arens et al. in *Applied Optics* 1987, **26**, 3846. Some recent results using the camera on IRTF are reported by Keto et al. in *Astrophys. J.* 1991, **374**, L29; 1992, **387**, L17; 1992, **389**, 223; and by Ball et al. 1992, **389**, 616. The appendix to Ball et al. 1992 gives an idea of one observing mode. The camera was successfully used on UKIRT last Semester and has been allocated time in Semester W.

Interested users should discuss any potential proposals with the Berkeley group and obtain their agreement to the collaboration well BEFORE submission of the application to PATT and should note that this is not a "common user" instrument and is currently only available courtesy of, operated by, and in collaboration with, the Berkeley Group. Because of the group's other commitments and its own research aims not all collaborative proposals may be acceptable. All proposals will be subject to the normal PATT review process.

Initial enquiries should be directed to:

Dr. C.J. Skinner
Institute of Geophysics and Planetary Physics
Lawrence Livermore National Laboratory
P.O. Box 808 L-413
Livermore, CA 94551-9900
U.S.A.

Fax: 010-1-510-423-0238
Tel: 010-1-510-423-0646
SPAN address: 6913::"skinner@tristan.llnl.gov"
INTERNET address: CBS%NSFNET-RELAY::GOV.LLNL.TRISTAN::SKINNER

UKIRT Service Observing

Just a reminder that the UKIRT service observing programme provides the opportunity to have short (about 2 hour) observations made on your behalf by UKIRT staff astronomers. If you are not familiar with the programme then please read the appropriate section in the UKIRTINFORM electronic help system, read the files DISK$USER3:[UKIRTSERV]UKIRTSERV.OBS and [UKIRTSERV]UKIRTSERV.HOW on the ROE STARLINK VAX, or e-mail your questions to UKIRTSERV at ROE. If you would like to be put on our mailing list and receive details of schedules, deadlines and instrument availability send your e-mail address to UKIRTSERV on the ROE STARLINK VAX (UK.AC.ROE. STAR).

Please remember to tell us if you complete your observation during a normal PATT run, or wish to withdraw it for other reasons, so we can delete it from our target list. Also we would be pleased to know when and where you publish your data, so we can keep our files up to date.

Schedule for Semester W

The schedule is not available as we go to press.

Report on Semesters U and V

This report covers the final 2 nights of Semester U and 8 of the 9 nights in Semester V. Since the last report 49 applications have been received (including some for Semester W), showing the continuing demand for service observing.

Weather during the period was quite good, with only two nights lost. Some of this was recovered during AIC time and so we have continued to maintain high productivity. A total of 45 programmes were attempted of which 33 were completed and 7 partly completed. The remainder were ongoing monitoring programmes.

Amongst the scientific achievements of the programme in recent months has been IRCAM observations to help interpret the CGS4 observations of high z radio galaxies reported in the last newsletter by Eales and Rawlings. The PIs report that images taken in February and March Service time have already been used in a paper submitted to Nature.

In our own Galaxy Malcolm Coe and others from

the University of Southampton report that they have used CGS4 2.0-2.5 micron spectra of Be/X-ray binaries obtained in service to investigate the strong hydrogen recombination lines, especially Brackett Gamma and higher order Pfund series. Since these systems are strong IR sources from the free-free emission in the circumstellar disk around the Be star, the strength and ratio of the newly observed lines enables them to determine the temperatures and optical depths in this disk. The current observations indicate the presence of a much cooler region to the disk than was previously suspected. This information is important in helping them to understand how the neutron star partner will accrete material from this disk and hence produce the observed X-ray emission.

In a separate programme Andrew Norton, Malcolm Coe, Sarah Unger (also from the University of Southampton) with Bruce Margon and Drew Phillips (University of Washington) report that using a combination of UKIRT/IRCAM service time and observations with the KPNO 1.3m telescope, they have performed a comprehensive infrared imaging survey of twenty nine radio sources which were first detected by the UBC radio patrol survey of the galactic plane. The sources in the sample are the subset of objects which were mapped with the VLA by Duric and Gregory. Since other sources in the original variability survey have been shown to be associated with unusual galactic X-ray and gamma-ray sources (i.e. Cas Gamma-1, Cyg X-3, LSI+61 303, 4U2316+61), the aim of this work was to make the first steps at discovering whether the remaining radio variables represent a hitherto undetected sample of faint, unusual X-ray binary stars.

As a result they detected infrared sources coincident with seven of these radio objects and have varying degrees of confidence in their status as true counterparts. The infrared objects are typically far redder than surrounding stars in the same fields (J - K~2.5) and are generally invisible on the optical sky survey plates. In addition to this, as a result of scanning the POSS plates, they have uncovered optical candidates coincident with eight radio positions. Most of these optical sources are close to the plate limiting magnitudes and only two objects are common between the sets of infrared and optical candidates. Further optical spectroscopic observations of all the candidates will follow, allowing us to determine whether they constitute a sample of galactic or extragalactic sources.

Finally, modesty will not prevent me from mentioning that service time was used by John Davies and Mark Sykes (IAUC 5480) to obtain JHK photometry (and subsequently CGS4 spectra) of the newly discovered outer solar system asteroid 1992AD. This revealed that the object was much redder than expected and suggested that the object's surface might be covered by a mixture of complex organic molecules and may imply a connection between it, comets and the small outer satellites of the distant planets. Since the asteroid had only been discovered 2 months earlier this shows the usefulness of a flexibly scheduled system for targets of opportunity.

We note the following publications using Service data, please let us know if you have published recently.

E. Churchwell et al., 1992, "The Wolf-Rayet System WR147: A Binary Radio Source with Thermal and Nonthermal Components." *ApJ*, 393, 329.

P. Eenens and P. Williams, 1992, "An Infrared View of Wolf-Rayet WC Subtypes - II. Abundances in Stratified Winds." *Mon. Not. R. astr. Soc.*, 255, 227.

M.H. van Kerkwijk et al., 1992, "Infrared Helium Emission Lines from CYGnus x-3 suggesting a Wolf-Rayet Star Companion". *Nature*, 355, 307.

M. Shaw, A. Tzioumis, A. Pedlar, 1992, "The Near IR and Milliarcsec Structure of PKS1345+125". *Mon. Not. R. astr. Soc.*, 256.

Observers and TOs who obtained data for service users included; Joel Aycock, Colin Aspin, Mark Casali, Ian Coulson, John Davies, Tom Geballe, Dolores Walther and Thor Wold. Kevin Krisciunas assisted with data reduction. Thanks to them and to our assessors.

John Davies
ROE

Successful UKIRT Applications for Semester W

PATT No	Principal Investigator	Nights Awarded	Title of Investigation
3	Leggett	3	A spectroscopic study of low-mass stars
6	Hough	2	Magnetic field geometries in stellar outflows
7	Hough	4	Spectropolarimetry of solid state features
8	Hough	3	Optical and infrared polarization of ultraluminous IRAS galaxies
9	Schild	3	Search for H_3^+
13	Walther	2	NIR Polarimetry of NGC2071IR
15	Geballe	1	Standards for CGS3/5
17	Rawlings	5	Near-IR lines in $z > 2$ radiogalaxies
24	Browne	4	The inner regions of quasars
25	Roche	2	Spectropolarimetry of SSV 13
28	Doyon	3	IR spectroscopy of NELGs
30	Wright	3	3.3 μm emission in galaxies
32	Wright	2	Spectroscopy of NGC253
33	Geballe	2	CO and H_2 lines in Orion
34	Emerson	4	High res midIR mapping of low-mass YSOs in Taurus-Auriga
35	Emerson	2	Solid CO towards icy low-mass YSOs in Taurus
36	Lawrence	3	How many high-z radio galaxies are quasars?
37	Barlow	4	The mineralogy of circumstellar dust
40	Sandford	2	CO_2 and CH_3OH in dense molecular clouds
44	Evans	over-ride status	Nucleation sites in novae
45	Naylor	3	Is CK Vul faint?
47	Jameson	3	IR spectra of low mass stars and brown dwarfs in the Pleiades
48	Rosen	3	IR spectroscopy of RE1149+28 & RE0751+14
51	Glazebrook	4	Deep infrared-selected redshift survey
52	Hoare	3	Evolution of BN object winds
53	Ward	2	IR spectropolarimetry of NGC1068
54	Ward	2	Excitation and reddening in nearby radio galaxies
55	Johnstone	3	Pressure in gas around $z \sim 2$ quasars
56	Walton	3	The formation of PN: 2μm spectroscopy
62	Gear	1	Polarimetry of XBLs
63	Lumsden	2	Cometary compact HII regions - bow-shocks or blisters?
64	Puxley	3	[FeII] as an indicator of supernovae rates in starbursts
66	Davies	1	Spectrally continuous recalibration of standard stars
67	Puxley	3	Spatial distribution of ionizing sources in starburst nuclei
70	Adamson	1	HDO and H_2S in Taurus
71	Adamson	1	Infrared DIBs
72	Adamson	3	4.5 - 4.9 μm spectroscopy of Taurus sources
73	Dunlop	3	IR imaging of milli-Jy radio galaxies
74	Wells	3	Velocity dispersion in starbursts
75	Brand	3	Physics of PDRs
77	Brand	3	The structure of shocks in OMC-1
83	Broadhurst	2	Near-infrared properties of IRAS galaxies
84	Waters	3	IR spectroscopy of post-AGB stars
85	Graham	4	Mid-IR images of proto-planetary nebulae
86	Jernigan	3	10 & 20 μm IRAS galaxy imaging
87	Tinney	3	HR diagram for lowest mass stars
96	Chandler	3	High excitation CO emission from YSOs
98	Isaak	4	Stellar seismology of Procyon

JCMT News

Expected Availability of JCMT Instruments during Semester X. (February 93 - July 93)

Introduction

Semester X (1 February 1993 - 31 July 1993) instrumentation on the JCMT is summarized below.

In the interest of saving space in the Newsletter and because there are no major changes to report, only brief descriptions are given below. Additional details can be found in the most recent issue of 'The James Clerk Maxwell Telescope: A Guide for the Prospective User', which is available through the JCMT Section of the Royal Observatory Edinburgh, by contacting the JCMT Group at the Herzberg Institute of Astrophysics in Canada, or from the Joint Astronomy Centre in Hawaii.

Spectral Line Observations

'A Band' Instruments

Receiver A2 was successfully commissioned in March 1992, is a single-channel SIS receiver and will be available to users as the default A band instrument. The tuning range covers 218 GHz to above 280 GHz. The receiver SSB noise temperature is 150K or better. The beam efficiency is around 0.7 with a slightly elliptical beam (21.5" x 20").

Receiver A1 is available only as a backup to RxA2. The receiver is in storage and may be brought on line within a couple of days. Users should not specifically aim to use this instrument without prior consultation with JAC staff.

'B Band' Instruments

Receiver B3(i) is also a single-channel SIS receiver. It may be tuned over the range from about 310 GHz up to 380 GHz, although the extremities of the band have yet to be fully explored. The DSB receiver temperature response is not constant with frequency, and ranges from a best value of near 140 K at 355 GHz to ~265 K at 330 GHz. On the sky, SSB system temperatures below 600 K have been obtained under good conditions.

The local oscillator system of B3(i) permits frequency-switched observations, with a maximum practical switch of +/- 50 MHz.

Receiver B2 is a dual-channel Schottky mixer system covering the range 330 to 360 GHz. The system temperatures obtainable on the sky under good conditions are between 1500 and 2000K throughout this band. This instrument is to be used only as a backup to RxB3i, or as a substitute if, for technical reasons, the SIS receiver cannot be present in the observing cabin.

'C Band' Instruments

Receiver C1 is a dual-channel 'hot electron' bolometer system designed for observations of the CO J=4→3 (461.04 GHz) and neutral carbon $^3P_1$-$^3P_0$ (492.16 GHz) lines. For the form of mixing used the practical single-sideband IF bandwidth is a little less than 2 MHz and it is necessary to 'sweep' the local oscillator frequency across the line to obtain a spectrum. Typical receiver temperatures are better than 800K at 461 GHz, and about 1300 K at 492 GHz for each mixer, or about 550 and 900K if both mixers are used at the same frequency. Under reasonable sky conditions, this leads to total system temperatures of ≈3000 and 7000 K per channel, or 30000 and 70000K respectively for a 50-channel spectrum.

Receiver C2(i) is a single-channel SIS receiver which will cover frequencies from 450 to 500 GHz, possibly with a DSB receiver temperature of 500 K. It is scheduled to be commissioned in October 1992 and thus should be available in Semester X if all goes well. Proposals are invited to use the receiver in Semester X, but the acceptance depends on the results of the commissioning tests.

Receiver 'G'

This receiver is a single-channel Schottky device employing a laser local oscillator arrangement. Because of this fact, only certain discrete frequencies can be accessed, in particular in the regions around the CO J=6→5 and 7→6 lines at about 690 and 800 GHz respectively. Typical double sideband receiver temperatures range from 3000 through 4500 K; specifically, at CO(6→5) and ^{13}CO(6→5) receiver temperatures of 3000 and 3500 K are obtained. The resulting single-sideband system temperatures are extremely sensitive to atmospheric conditions, but are likely to be of the order of 55000K or more under practical conditions.

Receiver 'G' is on loan from the MPE group in Garching and observers interested in using it should contact either Prof. R. Genzel or Dr. A. Harris to arrange collaborative efforts.

Spectrometer Backends

Two spectrometer systems are available for use during Semester X.

The **Digital Autocorrelation Spectrometer (DAS)** was partially commissioned in January 1992, and is already being offered to users in a restricted (narrow-band) mode of operation. The DAS has 2048 delay channels having a total maximum bandwidth of 1 GHz in each of two inputs. It is capable of a wide range of configurations, with spectral resolutions of between 0.1 and 1.0 MHz. These configurations include dual-polarization observations for those receivers that permit it (RxA1 and RxB2). The widest bandwidth modes are useful only for receivers (again RxA1 and RxB2) with sufficient IF bandwidth. It is possible to observe several lines in the same passband in either sideband with high resolution.

Currently there is a problem with baseline matching between "sub-bands". This appears to be caused by crosstalk in the digitizers and a non-linearity in the total power detectors. Until a fix has been installed by NFRA, the DAS is recommended only for narrow bandwidth (high-resolution) observations (with single or multiple lines). This is expected to be fixed shortly.

AOSC is an acousto-optical spectrometer which offers a resolution of about 330 kHz and a total bandwidth of 500 MHz for a single IF channel. The AOS is intended primarily as a backup for the DAS.

Approximate rms sensitivities after 30 minutes' integration

A table of the calculated rms noise in Kelvin after a total observation time of 30 minutes (this assumes 15 minutes on source, 15 minutes on a reference position), for three different values of the atmospheric transmission was included in the previous Newsletter. It will not be reproduced here.

Continuum Observations

UKT14

The UKT14 bolometer system will be available during Semester X with filters for observations at 2, 1.3, 1.1, 0.85, 0.8, 0.75, 0.6, 0.45 and 0.35 mm. The aperture of the bolometer can be adjusted between 21 and 65 mm. Sensitivities range from typically 0.3 Jy/$\sqrt{}$(Hz) to 10 Jy/$\sqrt{}$(Hz) or more under good photometric conditions, as given in the previous Newsletter in greater detail.

UKT14 polarimeter

The Aberdeen/QMW polarimeter will be available during Semester X as an optional accessory for the UKT14 bolometer system in step and integrate mode, and (possibly) also continuous rotation mode. The effective NEFD of the polarimeter-plus-UKT14 combination is slightly worse than NEFD(p) = 2xNEFD/P, where P is the degree of polarization of the source and NEFD is that given above (Table 2) for the filter/waveplate in question. Observations are possible at 1100, 800, and 450μm. Additional information appears in the article by Sye Murray in the JCMT-UKIRT Newsletter of August 1991 (p. 19), and in the 'Guide for the Prospective User'.

Henry Matthews
JAC, Hilo, Hawaii
(HEM@JACH.HAWAII.EDU)

JCMT Allocations — PATT TAG Report for Semester W

The PATT meeting for Semester W was held at the De Vere Hotel in Coventry, UK on 10th and 11th June 1992.

Applications to be considered:

U.H. applications	:	7
Applications with OTH PI	:	38
Applications with UK PI	:	36
Applications with CDN PI	:	26
Applications with NL PI	:	7
TOTAL	:	114

UK/(UK+CDN+NL) =52%
CDN/(UK+CDN+NL) =38%
NL/(UK+CDN+NL) =10%

6 of the 7 UH applications were awarded time by the UH TAG.

Last Semester (V) the number of applications for OTH:UK:CDN:NL were respectively 14:44:23:9. This Semester has seen a marked increase in the OTH category.

No of applications requiring line obs	:	61
No of applications requiring cont obs	:	58

Several applications require both line and continuum obs.

16-hr nights requested to PATT	:	279
Nights available for PATT science	:	127.5

Oversubscription = 2.15

Last Semester the oversubscription was 1.72.

PATT awards (in 16-hr nights)

No of nights in Semester W	:	184.0
For engineering/commissioning	:	38.0
Given to Univ. Hawaii (10%)	:	14.5
For Director's discretionary use	:	4.0
Nights available for PATT science	:	127.5

Awards by country paying salary of PI:

No of nights awarded to OTH	:	17.0
No of nights awarded to UK	:	60.5
No of nights awarded to CDN	:	28.5
No of nights awarded to NL	:	21.5

UK/(UK+CDN+NL) = 55%
CDN/(UK+CDN+NL) = 26%
NL/(UK+CDN+NL) = 19%

Awards by JCMT formula:

No of nights awarded to OTH	:	19.8
No of nights awarded to UK	:	60.4
No of nights awarded to CDN	:	27.2
No of nights awarded to NL	:	20.1

UK/(UK+CDN+NL) =56%
CDN/(UK+CDN+NL) =25%
NL/(UK+CDN+NL) =19%

Hopefully that is the last time I have to calculate the JCMT formulae! For those not familiar with the JCMT formulae, the total time requested is divided amongst the PI and collaborators. 50% of the time is awarded to the country paying the salary of the PI. The remaining 50% is divided equally over ALL investigators (including the PI). The difference between this method and by just allocating all time directly to country paying salary of PI is slight as can be seen from the figures above.

Instrument distribution:

Observing time requesting UKT14	52%
Observing time requesting RxA	18%
Observing time requesting RxB	24%
Observing time requesting RxC	6%

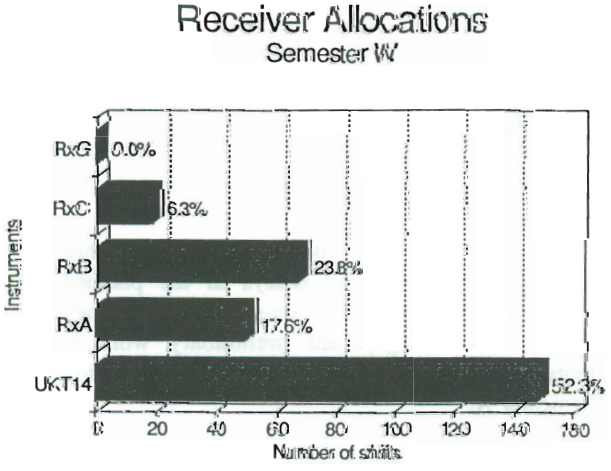

Confidence has returned to the RxB band instrumentation and the requests for time have increased. By default all observers will use RxB3i unless for technical reasons this instrument is unavailable in which case RxB2 should be offered.

Once RxC2i is commissioned it is likely that time requested for this band will increase significantly. In the interim RxC1 remains operational. Installation of this instrument means that RxB3i must be removed from the cabin.

All the RxG applications came in the OTH category. Only a small number of nights were awarded and the MPE Group declined the offer to use the JCMT this Semester.

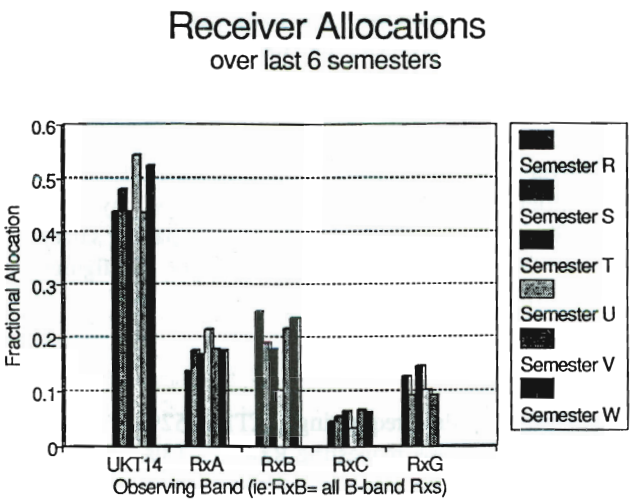

Long Term Projects:

One application (MW92: Ward-Thompson) was awarded long term status with 7 shifts being awarded this Semester and a further 7 shifts in Semester X.

Engineering and Commissioning:

The engineering and commissioning time has increased as a result of delays in the planned engineering schedule due to un-planned emergency repair work. Significant preliminary work is required before SCUBA is commissioned during Semester X.

Service Time:

This is developing in a reasonably progressive fashion for all partners. Wider distribution of the announcements of opportunity were called for. More use should be made of service mode observations wherever small quantities of data (up to 1 shift's worth) are required.

Allocations for Semester W are:

CDN	:	9 shifts allocated
NL & UK	:	8 shifts each allocated

The TAG awarded single shift observations to 2 applications which are to be attempted in service mode.

Changes in Assessments Procedures:

There are to be changes in the assessment and allocation procedures for at least the next couple of Semesters. This process has been delayed from the previous Semester. Applications from each partner country will be scientifically assessed by a TAG set up within that country. Applications with a PI from the OTH category will be assessed by all 3 partners unless a collaborator belongs to a partner country then the application will be assessed as coming from that partner. The partner TAGs will allocate shifts in priority order with guidelines set down about 1st availability, etc. At the next PATT meeting the Chairpersons of each TAG will meet with some representatives from the JCMT (Director, Scheduler, Tech Sec) to organise the final allocations.

Potential applicants for observing time in Semester X should check to ensure their applications are mailed to the correct establishment.

Graeme D. Watt
ROE
JCMT PATT Technical Secretary

News from JCMT Board

The JCMT Board held its eleventh meeting on May 18-20 in Hawaii. In addition to the formal meeting, the Board visited the JCMT and the Keck Telescope; received scientific presentations on the work of the JCMT; and met informally with JCMT staff and their families.

The Board warmly welcomed the selection of Professor Ian Robson of the University of Central Lancashire (formerly Lancashire Polytechnic), UK to be Director of the JCMT. He expects to take up the post in late 1992. The Board also thanked Dr Richard Wade for his considerable contributions to the JCMT during the past 30 months.

The Board proposes to issue reports from its meetings from time to time in the JCMT Newsletter. These will not normally report in detail the standard business dealt with by the Board, but will highlight items of specific interest. At the May 1992 meeting, the Board discussed the draft Instrumentation Development Plan presented by the recently appointed Head of the JCMT Receiver Programme, Dr Adrian Russell; it is hoped that a report on this may be issued at a later date. The Board also agreed a one-year trial of a new scheme for the allocation of time on the JCMT; and approved the creation of a JCMT Advisory Panel as a successor to the JCMT Users' Committee. Further information on these two items is given below.

Trial Scheme for Allocation of Observing Time on the JCMT

1. Introduction

1.1 The JCMT Board agreed at its meeting in May 1992 to implement a trial scheme for allocation of observing time on the JCMT. The principles of the scheme and the instructions for applicants are detailed below. Although the University of Hawaii is a Partner in the Tripartite Agreement, it deals separately with the allocation of the share of telescope time assigned to it. The trial scheme therefore applies to applications from the three Parties to the Agreement - the UK, Canada and the Netherlands - and to International applications (those not from the UK, Canada, Netherlands or University of Hawaii).

1.2 The trial will be for two Semesters, X and Y, starting with allocation of telescope time from February 1993. It will be reviewed, and a report presented to the Board after the allocation of Semester Y time in October 1993, by the International Time Allocation Committee (see section 4 below) after informal consultation with the national Time Allocation Groups (TAGs) and communities. The Board will consider at that time what is the most appropriate procedure for the allocation of the JCMT time in the longer term.

1.3 Canada, the Netherlands and the UK will each establish and run a national TAG, which will assess national proposals on the grounds of scientific merit and report to an International Time Allocation Committee (ITAC), which will make the final time allocations. The nationality of a proposal shall be regarded as determined by the principal applicant or the first from one of the Parties on the application.

2. Administrative Details

2.1 For the period of the experiment, the present PATT form shall be used by all applicants. Completed forms should be submitted to national addresses (see 'Instructions to Applicants', below.

Procedures for Handling Applications for Time on the JCMT during the Trial Period (Semesters X and Y)

1. Instructions to Applicants

1.1 For the duration of the trial, all applicants should use the standard PATT application, copies of which may be obtained from the national TAG.

1.2 Applications for JCMT time should be submitted to the national TAG of the Principal Investigator (PI) or, if the PI is not from one of the three Parties, to the national TAG of the first named co-investigator on the application who is from one of the Parties. International Applications (those with no applicants from one of the Parties) should be submitted to the UK national TAG.

1.3 Addresses to which applications should be sent are:

UK:

PATT Secretariat
Polaris House
North Star Avenue
SWINDON, SN2 1ET

Canada:

JCMT Time Allocation Group for Canada
c/o Director General
Herzberg Institute of Astrophysics
National Research Council of Canada
100 Sussex Drive
Room 2003
Ottawa
Ontario K1A 0R6
CANADA

Netherlands:

JCMT Program Committee
c/o Dr Frank Israel
Leiden Observatory
P O Box 9513
2300 RA Leiden
NETHERLANDS

The deadline for these applications is now 21st September, 1992, in order that they can be collated by 30th September.

JCMT Advisory Panel (JCMTAP)

The JCMT Advisory Panel (JCMTAP) is set up by the Board to advise the Board and the JCMT Director on the scientific programme and priorities for the JCMT; the strategy and priorities for the scientific development and maintenance of instrumentation and associated enhancements for the telescope, including requirements for data reduction, software packages and archiving; the current operations of the telescope and its instrumentation and software; the overall strategy for the future operation and exploitation of the JCMT (eg the application of remote observing); to consider such other matters as may be referred to it by the JCMT Board; and to bring to the attention of the JCMT Director or the JCMT Board, such other matters as may seem appropriate.

It will liaise regularly with appropriate bodies, in particular those responsible for the allocation of telescope time, and with the JCMT user community. Each Partner will determine the mechanism by which its representatives obtain the views of its users.

There will be nine members of the Panel, four nominated by the UK, two by Canada, two by the Netherlands and one by the U of H. It is expected that members will normally be users of the JCMT. In addition, meetings will normally be attended by the JCMT Director or his/her representative, who may, by agreement with the Panel Chairman, be supported by such additional staff as he/she considers necessary.

Meetings will normally take place twice a year, no more than 6 weeks before each meeting of the JCMT Board, though the Board recognises that there will be advantages from time to time in having meetings of the Panel adjacent in time to those of the Board. The Panel will report regularly to the JCMT Board, including advising the Board of any recommendations it makes to the JCMT Director.

Membership of the JCMT Board (as at 20 May 1992)

Dr D C Morton, Herzberg Institute of Astrophysics, Canada Chairman)
Professor E I Robson, University of Central Lancashire, UK (Vice Chairman)
Professor H R Butcher, Netherlands Foundation for Research in Astronomy
Professor W B Burton, Sterrewacht Leiden, The Netherlands
Dr I F Corbett, SERC, UK
Dr D N B Hall, University of Hawaii, USA
Dr W H McCutcheon, University of British Columbia, Canada
Professor K A Pounds, University of Leicester, UK
Professor D A Williams, UMIST, UK

The UK has nominated **Dr M J Griffin** (QMW) to succeed Professor Robson, whose term of office ends on 31 August 1992. Professor K A Pounds will take over the role of Vice Chairman.

Rowena L Sirey,
Secretary, JCMT Board

Successful JCMT Applications for Semester W

PATT No	Principal Investigator	Shifts Awarded	Title of Investigation
5	Hummel E	2	CO(3-2) in centre of NGC4631
6	Waters L B F	6	Mm obs of IRAS bright Be stars
8	Becklin E E	2	Dusty disks around Eps Eri & Tau 1 Eri
9	MacDonald G H	2	CH3CN mapping of protostellar objects
11	Weintraub D A	3	800um survey of dust disks around mag T Tau stars
12	Weintraub D A	4	450um mapping of selected PMS stars
17	Naylor D A	4	FTS spectroscopy of OMC
18	Davis G R	5	FTS spectroscopy of Jupiter & Mars
19	Welch W J	4	Study of gas acceleration process in MonR2 outflow
20	Gear W K	8	Broadband polarimetric obs of blazars
22	Saito S	1	Search for NH2 radical
24	Baas F	6	Mapping of star forming regions in W58
26	Hughes D H	5	Are cores of lobe-dominated QSOs same as RQQs?
28	Ivison R J	2	Obs of symbiotic stars RX-Puppis & H1-36
32	Matthews H E	8	Statistics of PMS disk masses and mol outflows
33	Matthews H E	2	The evolutionary status of MonR2
34	Seaquist E R	4	Mm recombination lines in M82
35	Little L T	3	The nature of CS dense cores in L1630
36	Heaton B D	3	Investigation of the evolution of luminous YSOs
37	Little L T	4	Search for CO(6-5) in primeval gal IRAS10214+4724
39	Barlow M J	6	Observations of Vega-excess stars
40	Ceccarelli C	2	Photometry of cold young low-mass IRAS sources
41	Moriarty-Schieven G H	3	Circumstellar environ & outflows from low-lum protostars
48	Longair M S	4	Study of dust & SF in high redshift radio gals
49	Mathieu R D	3	Evolution of CS disks in young binaries
51	Moore T J	1	Mutual evolution in CO outflows & IR refl nebulae
52	Avery L W	6	Search for Mg-bearing mols in IRC+10216
57	Fich M	3	Differential comparison of H2 & CO PD regions
58	Fich M	4	Detailed study of a spectacular molecular outflow
63	Mitchell G F	4	Testing shock models in IC443
71	Dent W R F	5	Relationship between optical and molecular jets
72	van Dishoeck	10	Chemical evolution of W3 molecular cloud
74	Lindsey C A	3	Mm to cm observations of the sun
76	Roche P F	6	Magnetic field structure in Orion
80	Greaves J S	3	Test of SF theories using CI maps of Orion radical reg
82	Lawrence A	7	Energy distribution of ultraluminous IRAS galaxies
83	White G J	6	460-490GHz survey of Orion
84	Richer J S	5	HiFi cont imaging of Orion B cloud core
85	Padman R	4	Dust around binary YSOs in Taurus
86	Padman R	5	CO mapping in L1221 & L1262
88	Minchin N R	4	Mag field structure around outflow sources
89	White G J	3	Understanding gas excitation in L1551
90	White G J	3	Shock excited gas in IC443
91	Hills R E	4	Search for C+ emission from high redshift quasars
92	Ward-Thompson D	7	The collapse of pre-stellar cores
93	Andre P	4	Comparative study of new class of extremely YSOs
95	Richer J S	5	Search for very fast CO jets coincident with HH objects
97	Richer J S	2	Phys cond of shocked gas in bipolar outflows
100	Israel F P	11	Molecular cloud ring in NGC7331
101	McHardy I M	5	Shocked jet models for blazars

Successful Applications for Semester W

PATT No	Principal Investigator	Shifts Awarded	Title of Investigation
102	Feldman P A	3	Very high excitation SiO masers in evolved stars
103	Feldman P A	4	Methanol as probe of SF in ultracompact HII regions
105	Marscher A P	2	Origin of gamma-ray emission in quasars
106	Hough J H	2	Is Cen A really the nearest blazar?
107	Tamura M	3	Mag fields in protostars circumstellar disks
UH1	Ladd E F	6	Submm mapping of luminous embedded clusters
UH2	Ladd E F	6	Temp & density structure of protostellar envelopes
UH4	Sanders D	4	Mol gas properties of normal galaxy nuclei
UH5	Sanders D	5	CO mapping of nearby starburst/active galaxies
UH6	Owen T	3	Submm observations of B-Pic & Mars
UH7	Jewitt D	5	Cold matter in galaxy clusters

Summary of the mm-VLBI experiment in February 1992

From the JCMT point of view the VLBI experiment was a roaring success, but this does not necessarily mean that the overall experiment was successful. We don't know yet, because it will actually take about 6 months before the data are processed (including time to finish work on the processor enabling both Mark II and K-4 data to be reduced. Success is only secured by perfect operation of all participating telescopes -- JCMT, OVRO, and SEST -- and apparently the weather conditions were unusually poor at the two latter sites. It should also be noted that there were no short baselines in the experiment, and to date fringes at 230 GHz have only been obtained on short baselines.

We borrowed essentially everything we needed for the experiment, and bought waveguides and a high quality synthesizer. Our Canadian partners provided us with a phase-lock system and a hydrogen maser, the Japanese with a complete K-4 recording system and a GPS receiver. Berkeley loaned us an 8 GHz receiver and NRAO lent a 230 GHz test tone system. Onsala built a circular polarizer. We really needed every piece of equipment we had been collecting.

Almost everything arrived much later than expected. The 8 GHz receiver was expected a month earlier, and 4 days before the experiment, we still lacked waveguides and a new feed horn. The hydrogen maser toured around the US mainland for a couple of weeks, and as a consequence it never had time to stabilize (it usually takes about a month). Apart from a short period during the last night, the drift, as measured relative to the GPS receiver was large but constant, and we should be able to cope with it in the post-processing.

We only had two shifts for setup, and during that time we were not only supposed to erect the equipment, but also carry out a 2hr 8 GHz fringe test experiment. But again, we made it, even though it looked impossible. After we had the 8 GHz system set up mechanically, 12 hours ahead of the experiment, we could not to open up because the wind speed was too high! Eventually we were ready to align and astronomically tune in the system. We did a perfect job, and reached a new record, the lowest frequency ever used on JCMT. We did run a bit into Canadian service time, but they got compensation later on. Of course we later found out that OVRO had failed and the whole experiment had to be repeated 2 days later during a six hour gap in the schedule. During that time we managed to re-mounted the whole receiver and mirror system, make a rapid alignment, and lose the first integration, but we finally made it. Not as well collimated as hoped, but good enough for the fringe test.

The following day we tried to get the 230 GHz system on line. Sky conditions were poor during the day, and although the experiment was due to start at 2 pm HST, we decided to make sure that we had enough phase stability instead. We found that the 100 MHz reference from the maser was not clean enough but with a temporary rig through the rented HP syntheziser we obtained the quality we required, and by the time 3C273 was up (10pm), our primary target, we were ready to start. Although we spent most of the following day making additional alignment tests (again during sky conditions unsuitable for observing) this was essentially the setup used throughout the run.

Overall very little useable observing time was lost, somewhere between 4 - 8 hours due to work on the system, and another 2 - 4 hours due to rapid drift of the hydrogen maser (most likely due to sudden stress release in the quartz cavity). This is an acceptable fraction of the 66 hours available for observing. Most of the daytime was unuseable due to severe anomalous refraction. The time suitable for observations was in reality more like 40 hours, so we may have lost 25%, which does not sound all that great. But for a first experiment I think we did a wonderful job, and we want to repeat it and do even better.

I have learned my lesson though. Next time we want to observe at both 100 GHz and 230 GHz. The 100 GHz is crucial, both to ensure success from a technical point of view -- a magnitude simpler -- and from a scientific point of view -- good uv-coverage and a key frequency for the behaviour of AGNs. We will therefore have to start the work on acquiring a 100 GHz SIS-receiver, and hopefully a receiver which can be used for other astronomy as well.

Note that VLBI is very much a team effort, both at the observatory level as well as internationally. We had a great team at JCMT:

M. Inoue and Miyaji (from NRO, Japan)
T. Legg and J. Fletcher (HIA, Canada)

M. Wright (UC Berkeley)
G. Sandell, P. Friberg, F. Baas, C. Hall, R. Prestage, telescope operators and mechanical and other support staff from JCMT.

Each of us contributed to the "success" and without the technical backup from JAC, we could not have done it.

Goeran Sandell
JACH

JCMT Service Observing

Report for Semester V

The UK Service Observing programme was initiated in Semester V and in response to the announcements of opportunity transmitted over the STARLINK network eighteen applications were received. All were assessed for scientific merit and technical feasibility, the latter requirement resulting in one proposal being rejected as too difficult. The eight shifts allocated to the programme were scheduled in blocks of four, two and two in March, May and June respectively in order to give a wide sky coverage. The observations were carried out by JACH and ROE staff with the remote link from ROE being used on two occasions. Although three shifts were lost, principally to bad weather, useful data were obtained for 8 projects. Those projects which were not attempted or only partially completed remain in the programme and will be attempted at the earliest opportunity.

Arrangements for Semester W

The allocation for Semester W is again eight shifts which have been provisionally scheduled in two blocks of four in December and January. Applications will be invited by way of NEWS items on STARLINK at the appropriate times. Proposals can, of course, be submitted at any time by e-mail to REVAD::JCMTSERV.

Alex McLachlan
ROE

Secondary Mirror Focusing and Chopping Losses

Whilst I was working at the Center for Astrophysics in the spring of 1990 I wrote a simple ray-tracing/physical optics program to calculate the beamshape and gain of a Cassegrain antenna given various offsets of the secondary mirror and feed. Although this program was written with the antennas of the CfA submillimeter (sic) array in mind, it also works perfectly well of course for the JCMT. I have a version of the program running both here in Cambridge and at the telescope that can be used to look at the beam pattern — as an example, I show here some calculations of the gain loss (reduction in NEFD if you like) arising from chopping the secondary mirror.

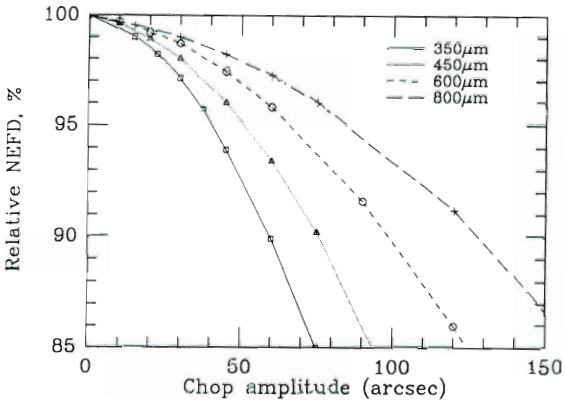

Figure 1.

The gain values are relative to those obtained for an on-axis untilted secondary mirror, with gaussian antenna illumination and 10dB edge taper (10% spillover). The antenna illumination pattern for UKT14 is not as well defined as with the heterodyne receivers — for normal "diffraction-limited" operation the taper is probably slightly less, in which case the gain loss will be very slightly greater for the same chop amplitude; for wider apertures however the losses will be lower. Figure 2 shows the same data as Fig. 1, but normalized to show that the loss is primarily a function of how many beams you chop off axis.

Most of the loss is coma, although there are also contributions from other aberrations. It can be seen that at 30 microns the loss of gain for a 45 arcsec chop amplitude (90 arcsec total chop) is about 5%, while at 800 microns the loss for a 90 arcsecond chop is less than 1.5 percent. A theoretical beam pattern at 450 microns with a 60 arcsec chop

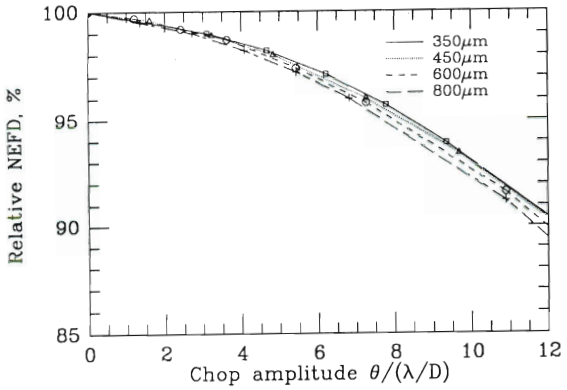

Figure 2.

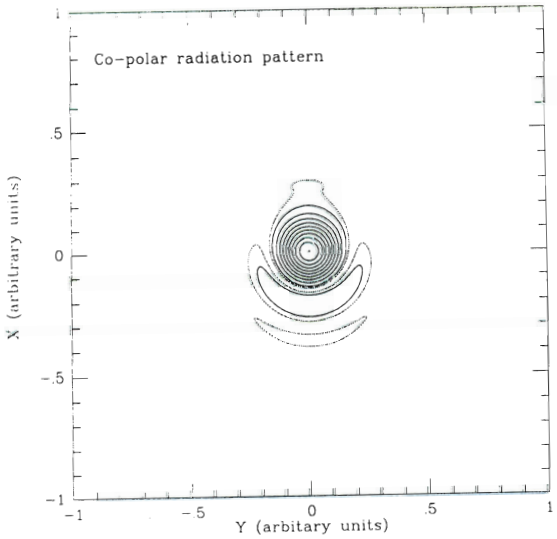

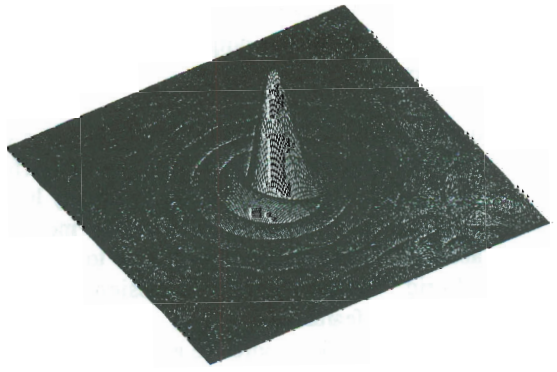

Figure 3.

amplitude is shown in Fig. 3 — cross-polarized radiation patterns can also be plotted.

As a final example, I show in Fig. 4 the loss of gain at two different wavelengths when the secondary mirror is "translated" in X or Y (as you do during an X-focus or Y-focus for example). The shift in the beam position is 28.8 arcsec per mm of X or Y shift, but this is automatically compensated for by the telescope control system. The loss is about 1% for a shift of 0.6 beam widths, and is essentially a quadratic function of focus offset. Thus at 800 microns a 0.25 mm error gives 1% loss; there is no point in wasting hours trying to get it right to 0.1 mm. At 450 micron the tolerance is reduced proportionally, but again, you need not set it any better than about 0.15 mm.

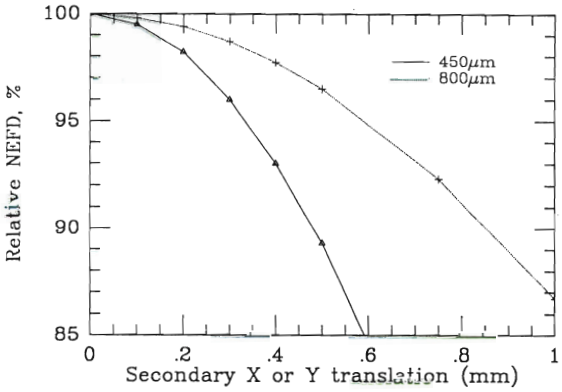

Figure 4.

If you are interested in using this program at JCMT, then both program and instructions can be found in the directory **jcmt::disk$data:[rachael.jcmt]**. Just type or print the file **AAA_READ_ME.TXT** for full instructions. I believe that the telescope currently uses a version of MONGO compatible with all the data files produced by JCMT_BEAM.

Rachael Padman

CAVAD::RP1
RACHAEL@UK.AC.CAM.PHY-RAVX

Frequency and Velocity Scales in SPECX

Introduction

Traditionally, radio spectral-line analysis programs have displayed velocities with respect to the Local Standard of Rest (LSR), using the radio definition of velocity. It is now possible to observe at JCMT using Heliocentric, Barycentric and Telluric velocity frames, and optical and relativistic velocity definitions, and SPECX V6.2 (now released to Starlink) contains the appropriate facilities for dealing with such data. Before describing what SPECX does, it is necessary to review, briefly, what is required (see also ref[1]). We all know that any relative velocity between source and observer gives rise to a corresponding Doppler shift in the received frequency. For *small* velocities, then, radioastronomers (who think in frequencies) write

$$\nu/\nu_0 = (c-v)/c = -v/c, \quad ...1$$

where v is the velocity *away* from the observer. Likewise, optical astronomers write a similar formula in wavelengths:

$$\lambda_0/\lambda = c/(c+v) = v/c. \quad ...2$$

Finally, it seems that extragalactic observers believe in special relativity, which of course tells us that:

$$\nu/\nu_0 = \sqrt{[(c-v)/(c+v)]}. \quad ...3$$

(ignoring the smaller doppler shift due to any transverse component of velocity). By a simple application of the binomial theorem, we can see that these are all equivalent for $v << c$. A problem arises because these equations are used in reverse to *define* a velocity, and this definition is often used where the approximations in (1) or (2) are inadmissable. Even the (special) relativistic formula applies only in *local* frames, which are not the same thing at all as distant cosmological frames. So none of these formula are "right".

Normally we reduce our velocities to one of a few commonly agreed standards: Radio astronomers prefer the Local Standard of Rest (LSR); extragalactic astronomers apparently prefer a Heliocentric system, whilst for some purposes, such as instrument or atmospheric diagnostics it may be the Telluric frame that is of most interest. Or indeed we may have some favourite other frame which is defined with respect to one of these "standard" frames. One that is used quite often is the source frame — for example, if we want the frequency scale to be that appropriate to a non-moving source we have to transform all telluric (observed) frequencies to a frame comoving with the source. In the case of Orion for example this is 9 km/s wrt the LSR, and few of us know the heliocentric velocity.

Thus our velocity scale is specified by four parameters:

i. The velocity transformation law.
ii. The rest frequency or wavelength used in the law.
iii. The standard frame, and
iv. The reference velocity expressed in that frame.

Here I use the general term "frame" to imply this full specification.

Observation and Display of Line Spectra

There are two separate issues. First, we need to *observe* such that the line of interest actually occurs within the passband of the instrument (normally, but not always, at the centre of the passband). For a heterodyne receiver we do this by adjusting the local oscillator frequency by an amount equal to the *total* doppler frequency shift expected for the line. Second, we then need to *display* the spectrum. Unfortunately, the spectrometer is back on Earth, at the telescope, so we need to map the I.F. frequencies of individual spectrometer channels onto velocity (or frequency) space in some other chosen frame. This 'display' frame need not necessarily be the same as the 'observation' frame. For example, whatever the observation frame, we may wish to display the output in one of several standard frames:

i. In the telluric frame, where the frequencies of spurious responses in the I.F. passband (for example) can be measured, and with any luck, disposed of. Or we may wish to measure absolute frequency in this frame to identify telluric (atmospheric) emission and/or absorption features.
ii. In the frame of the source (e.g., at a velocity of V_{lsr} offset with respect to the LSR frame itself), when we wish to measure the absolute

frequency of some spectral feature, in case it is a spectral line of some species other than the one we desired.

iii. In the LSR frame, if we want to determine a velocity to use for distance measurements within the galaxy.

iv. In a heliocentric frame for velocity determinations of external galaxies (I am told that this is the normal way of doing this.)

The solution adopted in SPECX is to view all calculations of velocity and/or frequency as a two stage process. In the first, the spectral header information is used to calculate the telluric centre frequency of the observation. That is, we deduce the true frequency as measured at the telescope of a signal appearing in the centre channel of the spectrometer. SPECX then produces an 'X-array' which contains, for each spectrometer channel, the telluric frequency corresponding to that channel. Finally, this array is transformed back to the display frame. By default the display frame is the same as the observation frame, which is encoded in the SPECX and GSD scan headers, but it may be changed to any other frame if you like.

To summarize: SPECX will normally display the data using the velocity frame in which it was observed; however you can use SET-VELOCITY-FRAME to select another frame, and optionally you can use SET-LINE-REST-FREQ to choose another reference frequency for the velocity transformation. Current options for frames include LSR, Geocentric, Heliocentric and Telluric, and you have a choice of Radio, Optical and Relativistic velocity laws. Because of the bewildering number of combinations of these variables, the header on the X-axis of the plot has been modified to give a full specification.

Complications 1: Displaying the other sideband.

The command CHANGE-SIDEBAND does the following: first, it calculates the telluric centre frequency. Then it adds or subtracts twice the I.F. (depending on whether the observations are in LSB or USB respectively). Finally, it transforms this telluric frequency to the nominal frame of the observation, files it as F_CEN in the scan header, and changes the sense of the frequency step in the spectrometer (F_INC). GSD spectra stored with storage task V6 or earlier do not have the local oscillator frequency stored, so SPECX instead asks you for the current sideband and I.F.; for V7 data or later SPECX can deduce these from the data in the GSD scan header.

Let us take a specific example. We have a R x B3i spectrum which is centred on CS 7-6 (rest freq. 342.883 GHz) in the lower sideband. The nominal I.F. is 1.5 GHz. In order to look at absolute "rest frame" frequencies, we set the display frame to be that of the source itself:

```
>> set-velocity-frame
Output in different vel frame? (Y/N) [Y]
Velocity frame? (TELLuric,LSR,HELIocentric,GEOcentric) [TELL] LSR
Velocity law definition? (OPTical, RADio, RELativistic) [RAD] RAD Velocity in new frame? (km/s) [ 20.0] vlsr
```

(see Fig 1). (There is a predefined variable "vlsr" equated to the actual value for the current spectrum, so we can quote this in response to the last query rather than looking up the actual value.)

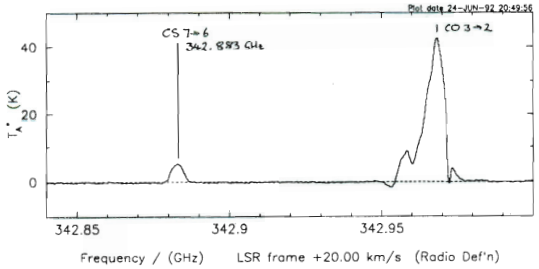


```
Scan  138  0138.001  M17        JCMT  Obs'd 13-APR-92 at 14:45:47(UT)
Map centre:  18 17 27.98; -16 13 24.00  Offset(R,D): (  27  -15) arcsec
Int'n time:  300.00 sec; Elevation: 53.3 deg; Vlsr:  20.0 km/s
Quad.  #pts. Cent.Ch  Rest Freq(GHz) Obs.Freq(GHz) Inc.freq(MHz) Tsys(K)
```

For an AOSC spectrum, we would now regrid to a linear scale (see next section for more details on this). Then we go ahead and change the sideband:

```
>> change-sideband
Local oscillator frequency not defined...
Current sideband? (U/L) [L] L
First i.f.? (GHz) [ 1.500000] 1.5
```

--- Header entries changed to other sideband ---
Don't forget to use SET-LINE-REST-FREQ to set the frequency of the line you wanted to look at — the old line will appear at large velocities!

As suggested, change the reference frequency to CO 3-2:

```
>> set-line-rest-freq
Receiver # 1  Line rest frequency? (GHz)
[ 0.000000] 345.795989
```

If we have done all this correctly we now get the absolute frequency plot shown below (Fig 2). A macro has been provided to do all this — just type I M A G E - F R E Q (this calls specx_command:image.spx).

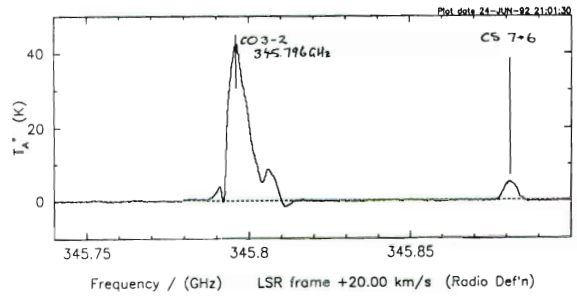

Scan 138 0138.001 M17 JCMT Obs'd 13-APR-92 at 14:45:47(UT)
Map centre: 18 17 27.98; -16 13 24.00 Offset(R,D): (27 -15) arcsec
Int'n time: 300.00 sec; Elevation: 53.3 deg; Vlsr: 20.0 km/s
Quad. #pts. Cent.Ch Rest Freq(GHz) Obs.Freq(GHz) Inc.freq(MHz) Tsys(K)

Complications 2: AOSC

It is well known that the frequency scales of Acousto-Optical spectrometers tend to be non-linear. To this end, the SPECX frequency calculation stuff contains a facility for correcting the frequency using a polynomial fit to the frequency error. For AOSC, the cubic term dominates, and the maximum error is about 0.6 MHz, but for somewhat complicated reasons, there is an *additional* zero-order (d.c.) term of some 11 or 12 channels, or about 3 MHz. The implication of this is that a line you might expect to come out in the centre channel (1024.5) of the spectrum will actually emerge some 3 MHz away, and to compensate for this the GSD header files correct the reference-frame observed frequency, F_CEN, appropriately. This makes the display work fine, but has implications for when we want to look at image frequencies (as will be shown in a moment).

To correct the frequency scale for AOSC data in particular, I have written a small macro, FRQFIX.SPX, which is kept in the "standard" command-files directory. It is invoked by the symbol LINEARIZE-AOSC-FREQ:

```
>> linearize-aosc-freq
FRQFIX> Linearization turned off — reset it? (Y/N) [Y] Y
OK, setting freq coefficients
FRQFIX> Regrid to uniform sampling? (Y/N) [Y] Y
 -- AOS frequency scale linearization applied --
First and last useful channels in input:  1  2038
Linearization has now been turned off!
```

Reset if another spectrum needs correcting

This macro in fact *also* removes the 3-MHz offset from F_CEN, instead adding it into the zero-order term of the correction polynomial, which simplifies calculation of the I.F. LINEARIZE also does various checks and tidies up the program flags. If you choose to REGRID the data at this point you transform the data to a truly linear scale (in current units). Otherwise the data will still display correctly, as long as you have the linearization turned on (set fcorrect=true or use SET-X).

If you now want to look at the other sideband of AOSC data, remember that the effective I.F. at the centre of the passband is not what you might think it is, but is actually 1.503 GHz (or 3.943 GHz for R x A1 or R x B2). If on the other hand you apply the LINEARIZE-AOSC macro the data will be regridded onto a linear scale *and shifted to the nominal channel.* In this case the I.F. is the standard 1.5 or 3.94 GHz. There is one Awful Warning: you cannot apply linearization to data *after* you have done a CHANGE-SIDE. That flips the spectrometer frequency scale, and so will apply the correction 'the wrong way round'. So after you have done a CHANGE-SIDE, make sure that linearization is turned off, either through SET-X or by typing "fcorrect=false".

I thank Per Friberg, Goeran Sandell and Chris Mayer for their help in untangling this mess, Louis Noreau for pointing out the need for other velocity frames and scaling laws, and Paul Feldman for bringing other infelicities in the velocity and frequency scaling to my attention. The system in SPECX V6.2 has been written from scratch, and so does not have 10 years of testing behind it; please bring any demonstrable faults to my attention. (I do not have Donald Knuth's confidence, and do not offer a steadily increasing reward for each bug found in my code.)

Efficient map-making

Finally, a brief note about map-making. People are making some really quite big maps. SPECX tries to hold the entire cube in virtual memory at one time, and in fact with various permutations of INTERPOLATE and ROTATE, may want to have up to 3 copies of the cube resident. If excessive paging is to be avoided, then it is desirable that all these fit into the available physical memory of the machine (the working set). The usual consequence if they do not is that the whole machine grinds to a halt, without any apparent error...

You can minimize the amount of virtual memory required by only mapping those spectral channels of interest. Use TRUNCATE (or DROP-CHANNELS) to dispense with spectral channels lying far away from the line; use BIN-SPECTRUM where you have higher resolution than you need. Even if you have plenty of memory to spare, you can greatly speed up the map-making process by using as few channels as possible. To reinforce this point, when you do an OPEN-MAP you are now asked explicitly for the number of spectral channels in the cube. You can also eliminate one cube from memory altogether by using 'interpolation-on-demand' (an option in INTERPOLATE-MAP), albeit at the cost of slightly increased time to make any particular map.

As noted in the manual, SPECX maps are really channel maps, and no information is stored in the header about individual spectra. Thus if you want to map data taken in the other sideband from that of the map header, or taken with a different spectrometer etc., you first need to INVERT, SHIFT, TRUNCATE etc. to get your spectrum into the right form. There is a new macro that does this automatically: it can be invoked by the command symbol CONVERT-TO-MAP-FORMAT (this macro is stored along with all the other standard macros in the directory with logical name "specx_command"). Just use this command before you ADD-TO-MAP to convert your current spectrum to the same frequency scaling etc. as the map header.

Reference

[1] Gordon, M.A., 1976, in *"Methods of Experimental Physics"*, vol 12-C, Chap. 6.1, (Astrophysics -- Radio Observations), Acad.Press.NY.

Rachael Padman

CAVAD::RP1
RACHAEL@UK.AC.CAM.PHY-RAVX

First Interferometric Fringes between JCMT and CSO

Discussions have been going on for some time about the possibility of linking together the JCMT and the Caltech Submillimeter Observatory (which is located about 160 metres away) to form an interferometer. A plan to do this was approved in November 1991 and events have moved quite rapidly since then. Optical fibres with especially high thermal stability were installed in the underground ducts between the two telescopes, an optical delay line was built and new phase-lock systems designed for interferometric use were developed. Many other elements such as software for the JCMT computer and hardware for interfacing to the DAS (which was used to correlate the signals) also had to be prepared. All these items came together on Mauna Kea early in June and after a week or so of frantic activity everything was ready for the first tests on 15th and 16th June. Unfortunately the weather was very poor - the first attempts were made through thick cloud and, not surprisingly, no fringes were seen. However, conditions improved a little and on the 16th, after some unsuccessful attempts on weaker sources, fringes were finally detected from the star U Herc in the "masing" water line at 321 GHz.

The visibility was however low and the fringes were not seen consistently. We do not yet know whether this was due to some problem with the equipment or a mistake in the software or whether it was just that the atmosphere was too unstable to give good fringes at that time. (Direction of arrival fluctuations - seeing - of around an arc second peak to peak would have smeared them out.) Nevertheless the fact that all the new systems basically worked correctly was very encouraging. We are now looking forward to the next set of tests which are scheduled for the beginning of September.

Richard Hills,
MRAO

John Carlstrom,
Caltech, Pasdena

Jupiter's Ring

One morning during a recent visit to JCMT (after the PATT observers had gone down) I decided to make some large-scale 'on-the-fly' maps of Jupiter using UKT14. The results, for three of the standard observing frequencies, are shown in Fig. 1. As usual the data were taken with secondary mirror chopping and passed through the phase-sensitive detector. This is the raw data (to show that the effect isn't a result of any fancy data processing) so you see two copies of each image, one positive and one negative. The splodge in the middle of each is Jupiter, but in every case one can quite clearly see a ring around it. In fact these rings are quite faint — from a few percent of peak at 350 microns, down to under 1 percent at 800 — and I had to turn up the contrast on the plots to get them to show up, which accounts for the 'burned out' appearance of Jupiter. Note that the diameter of the ring increases (linearly) with wavelength, while the intensity decreases.

So what are these rings? Well of course this is not really an astronomical phenomenon at all — what we are seeing is the far-out sidelobe pattern of the telescope, and that was what I was trying to measure. In fact we have known for some time that JCMT has an extended error pattern. It showed up clearly on solar scans made by Charlie Lindsey and Alan Clarke a couple of years ago. Alan did a model fit to his data that showed that a large fraction of the energy collected by the telescope comes from this extended pattern (at least it does when it is being heated up by pointing at the Sun). 1-D scans across Jupiter made by Per Friberg also showed the presence of this far-out lobe and John Richer and I analysed these. We then realised that the position of the lobe was exactly what would be expected from a defect in the surface that we have long known about from the 94 GHz 'holography' measurements.

When we measure the shape of the surface using the phase-recovery method (as described in the March 1988 JCMT Newsletter) we do in fact get a detailed map of the whole surface with a spatial resolution of about 6 inches. What is normally done is to make a fit of the best sets of adjustments to make to the panels, using the three adjusters on each panel, and then just look at a plot of the change to the surface that these adjustments will make. This limits the effective resolution to the size of a panel (about a metre). However if one looks at the *residuals* to this fit, i.e. the errors that one will not be able to adjust out, one sees a clear pattern, as shown in Fig. 2. When one compares this with the arrangement of panels it becomes clear that the problem is that the individual panels do not

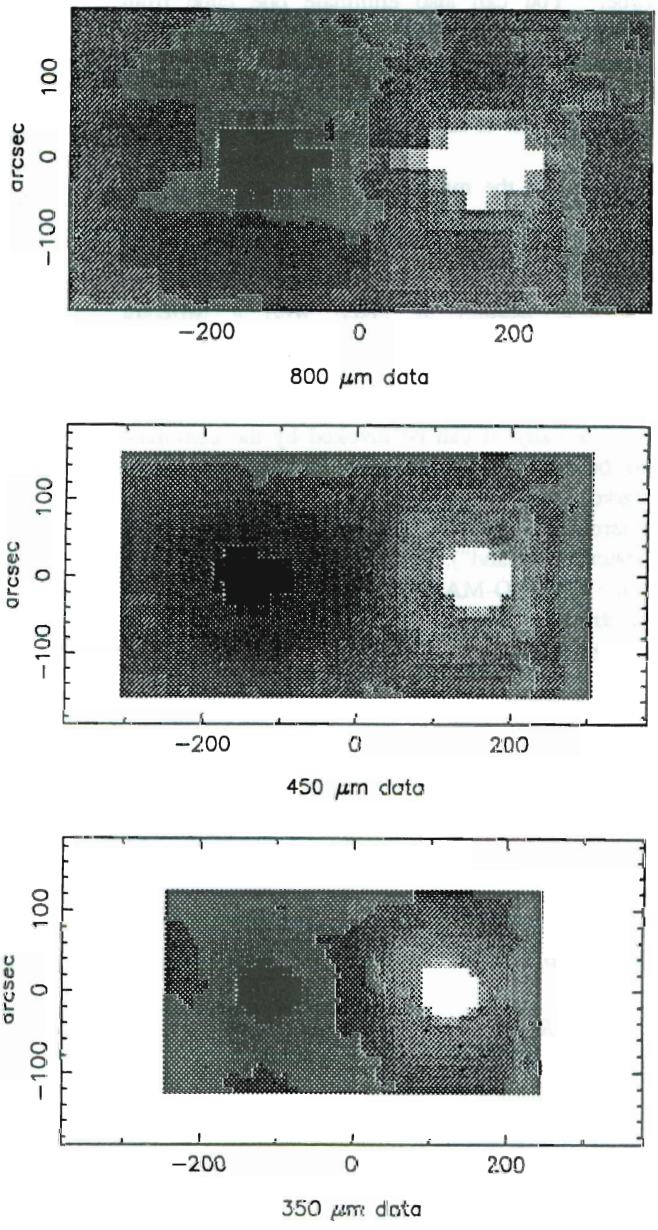

Figure 1. The raw data from some large-scale maps of Jupiter, using UKT14, taken with secondary mirror chopping and passed through the phase-sensitive detector.

have exactly the right curvature to match the curvature of the telescope surface. It turns out that either the panels are too flat or the dish is too deep. (We don't actually know which. Probably it is a bit of each. I suspect that the panels 'sprang back' a little when they were released from their moulds, but I also know that when we did the initial setting up of the dish using the laser measuring machine we did set it somewhat too deep.)

Now this mismatch produces an error in the surface which is a periodic function of radius. The period is the radial length a panel, almost exactly a metre, so the diffraction pattern produced will be a ring with an angular scale of 100 arc seconds (half a milliradian) at a wavelength of half a millimetre, just as seen. I have shown the Fourier transform of the residual error pattern in Fig. 3 to illustrate how well defined the pattern is. Taking this a stage further one can calculate the beam pattern that one would expect at 450 microns from the errors in the surface measured at 94 GHz, convolve it with an artificial Jupiter and I have plotted this predicted beam pattern alongside the real data (Fig. 4). I find the agreement rather impressive!

As already mentioned the ring is at quite a low level even at 350 microns, so it is not likely to cause problems with most observations. However, because it covers a lot of solid angle, the ring represents quite a large fraction of the total coupling of the detector to the sky. By summing the data in a series of rings of increasing radius I find that the ratio of the energy in the diffraction ring to that in the main beam (which also includes near-in sidelobes because Jupiter is so large) is 0.42

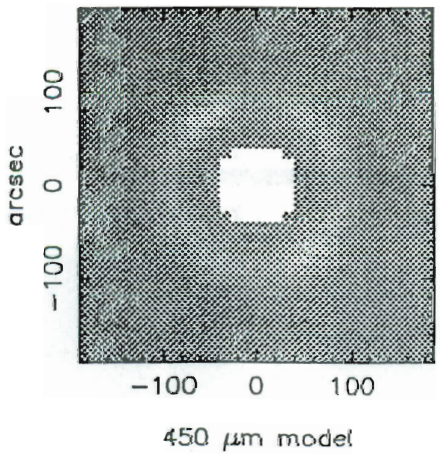

Figure 2. Residuals to the fit of the best sets of adjustments to make to the panels, unsing the three adjusters on each panel.

at 350 microns, 0.29 at 450 microns and 0.085 at 800 microns. These figures are consistent with an rms of about 18 microns for this component of the surface error. (This value is a little higher than what one gets by just looking at the holography data, which indicate that the periodic term has an

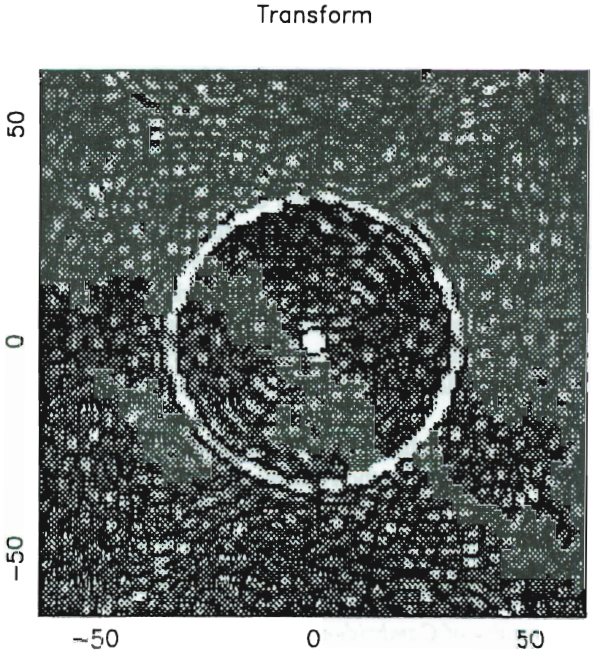

Figure 3. The Fourier transform of the residual error pattern illustrates the definition of the pattern.

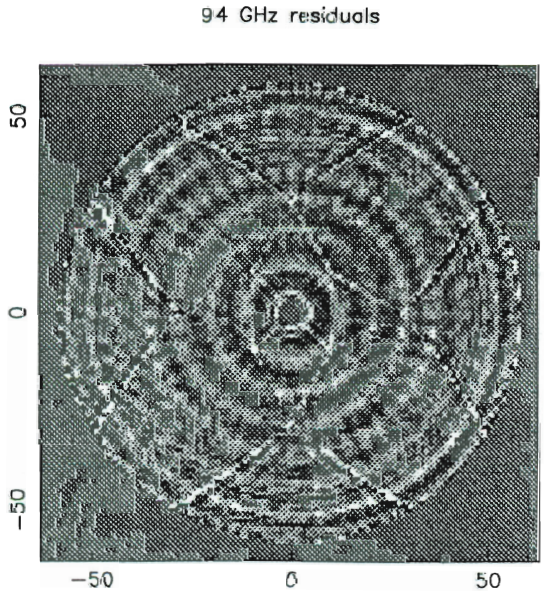

Figure 4. The beam pattern expected at 450 microns from the errors in the surface measured at 94 GHz.

rms of about 15 microns. Probably some other components of the surface error pattern are scattering energy into the region of the ring.)

This is quite a significant contribution to the overall surface error of the telescope. The good news is that in principle we can get rid of it by just resetting the dish to have a shallower curvature. The bad news is that we need to move it quite a long way — well actually the focal length only has to increase by an inch or so, which doesn't seem very far on a structure as big as JCMT, but it is somewhat outside the range of the electronically controlled adjusters we have on the panels. This means that we will probably have to fit shims under some of the adjusters or possibly even reset the backing structure. However it is obviously worth devoting some effort to this because there should be an improvement in observing efficiency of around 40% available at the highest frequencies.

My thanks to John Richer for his help with the data reduction and to Anthony Lasenby and many others for useful discussions.

Richard Hills
Department of Physics
University of Cambridge

The 'Inner' Error Beam of the JCMT

Elsewhere in this newsletter, Richard Hills has described recent measurements of the 'outer' error beam of the JCMT at 450 microns: using the large and bright planet Jupiter, Richard mapped the beam pattern on large angular scales (about 100 arcsec) and showed that it was quite consistent with the small-scale surface errors (which are due mainly to the scalloping of the panels). To complete this picture after the latest dish re-adjustment, I thought I'd show my latest maps of the 'inner' error beam (beam radii less than 40 arcsec) which were made in June this year. The power pattern on these scales is controlled by how well the the large scale surface errors (with a correlation length of a few metres) have been corrected by out-of-focus maps.

Mars is the ideal object for mapping the inner error beam, as it is bright and usually smaller than the main (diffraction) beam. The maps were taken with UKT14 at the end of one morning shift of PATT time, after my object had set, and Mars had a diameter of 5.4 arcsec at the time. The weather was extremely dry and stable (the CSO tau meter read 0.045) which enabled me to make large, oversampled maps at 450 and 350 microns; the chop throw was 40 arcsec. These raw data are the true beam response convolved with the planetary disc and the dual-beam function: I used DBMEM (MNRAS 254 165) to deconvolve the maps and make images of the beam pattern (Fig. 1). Unlike many deconvolution problems, this one is rather well behaved since we know that there can be no spatial frequencies in the beam below the diffraction limit and so can enforce smoothness in our reconstructions on this scale. (Incidentally, these

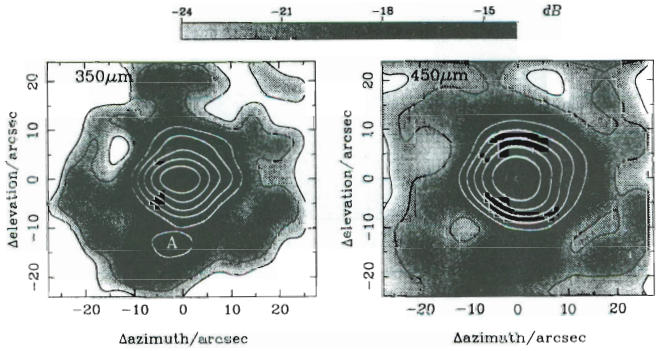

Figure 1.

derived beam maps can be used as the point spread function for deconvolution using DBMEM).

The 350 and 450 micron maps are displayed logarithmically, with contours at increments of -3dB from the peak response, and they have a signal-to-noise ratio of around 200. We can be sure that most of the features are real since they show up in both the 350 and 450 maps: of course, the sizes and positions of the features scale by (450/350) as we go from the 350 to 450 micron map, and they become fainter due to the smaller Ruze factor. The strongest sidelobe is labelled in the 350 micron map as feature 'A', and even this has a peak power response of only -13dB. Gaussian fits to these maps yield best-fit values of 8.8 x 6.5 arcsec (Azimuth x Elevation) at 350 micron and 9.5 x 8.5 arcsec at 450 micron. This elongation along azimuth is at least partly due to the analogue demodulation system used which has no blanking as the secondary chops from left to right. Digital demodulation with chopper blanking is needed to see just how much of this non-roundness is due to the demodulation and how much to the large scale deformations of the dish.

The best way to estimate the magnitude of the large scale errors is to find the integrated power in these beam models as a function of radius: this has been done in Fig. 2 (solid lines), normalising the total power to unity at a radius of 35 arcsec. In each case, the theoretical curves for a two-component axisymmetric Gaussian beam model is shown by crosses: these are not 'best' fits, but are consistent in that that the components' sizes are scaled by roughly 450/350 between the maps. The poor fit to the 350 micron profile near the origin is due to ellipticity of the true 350 micron beam.

At 450 micron, approximately 70% of the power within 30 arcsec is in the diffraction-limited main beam, with the rest in a Gaussian component of size 30 arcsec FWHM. This corresponds to an RMS surface error in the large-scale component of around 21 micron, and to a correlation length of the errors of 2.5 metres. To obtain the total surface error we should should add this in quadrature to the small scale errors discussed in Richard Hills' article. However, the bottom line is that the JCMT beam is in pretty good shape for high frequency mapping!

John Richer, MRAO

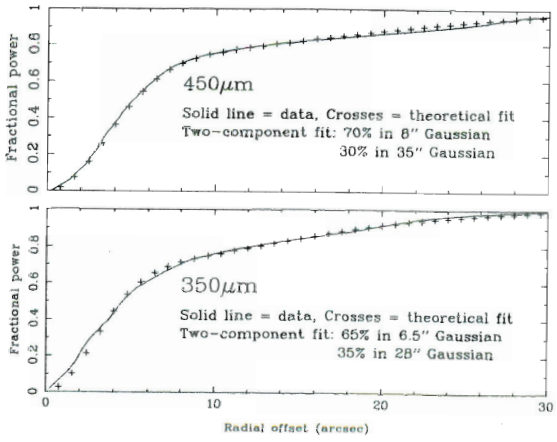

Figure 2.

New Results

The Berkeley mid-IR Camera

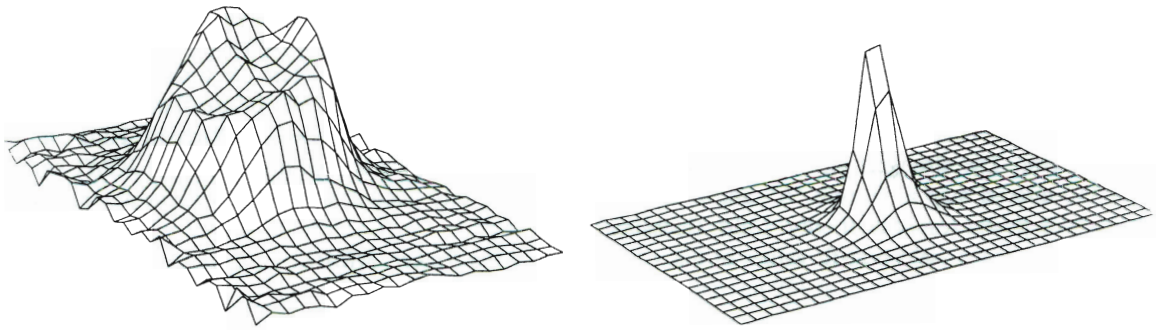

Discovery! Image of AFGL 2343 at 12.5 μm taken with the Berkeley/IGPP mid-infrared camera on UKIRT on June 6, 1992, at a pixel scale of 0.4"/pixel. AFGL 2343 is a high latitude supergiant (G5Ia) at a distance of ~1 - 3 kpc with a large IRAS excess at 12 μm (30Jy) and 25 μm (650Jy). A plot of the compact `stellar´ source, g Aql, is shown for comparison purposes. An extended dust shell is obviously present around AFGL 2343 and shows the exciting results that can be obtained in the mid-IR using instruments such as Berkcam.

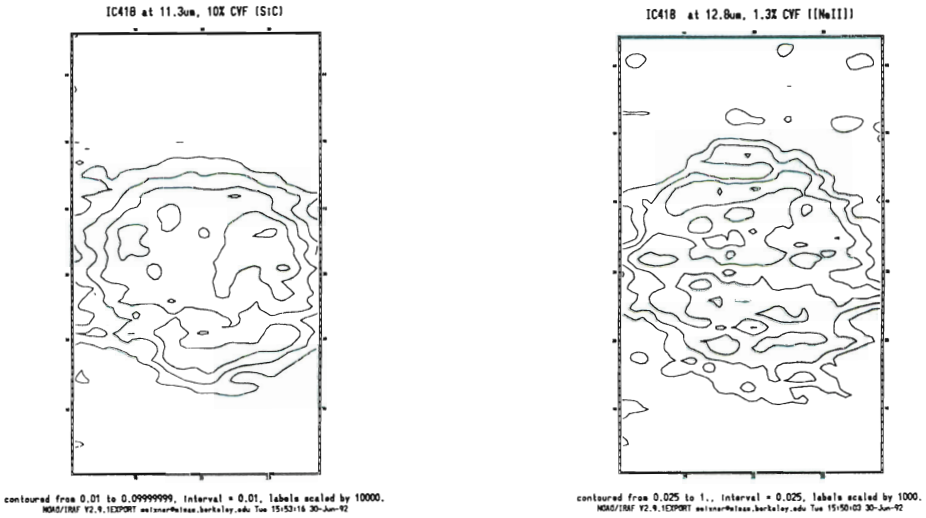

Images of IC418, a nearby young planetary nebula at 11.3 μm and 12.8 μm using the 10% and 1.3% CVFs respectively in Berkcam. The object is dominated by SiC emission at 11.3 μm while the 12.8 μm 1.3% CVF image samples the [NeII] line emission and probably traces the low excitation ionized gas component.

In all Berkcam images, North is to the right and East at the top.

A detailed discussion of these data will be given in a later issue.

Margaret Meixner
George Hawkins
Berkeley, California

Very Deep Imaging of Abell Clusters: Infrared and Visual-Infrared Colour Gradients of cD Galaxies

The largest galaxies in the universe, the cDs, can be found in the centres of rich clusters of galaxies. They are elliptical-like galaxies characterised by relatively flat surface brightness profiles; a central surface brightness that is lower than that of giant elliptical galaxies; an elongated shape in their outer regions with their flattening often aligned with the cluster. When the galaxy also contains a faint extended halo, it is properly called a cD galaxy (Matthews, Morgan & Schmidt 1964); otherwise it is called a D galaxy.

Several models of the formation mechanism have been made to explain these characteristics. It has been argued (e.g. Gunn & Tinsley 1976, Hausman & Ostriker 1978, Malumuth & Richstone 1984) that mergers, accretions and stripping in the cluster form the central galaxy. In this model it is unclear whether only the extended halo, or the whole cD is formed this way. A totally different scenario has been suggested by X-ray astronomers (e.g. Fabian & Nulsen 1977). Clusters usually are surrounded by huge X-ray haloes, and the cooling time of the gas in the centre is often shorted than a Hubble time. This has led to the suggestion of cooling flows of gas towards the centre. Calculations show that some clusters have cooling flows of several hundreds of solar masses per year, and in such a way the cD could be built up over a Hubble time. Small amounts of current star formation have been detected in some cDs (e.g. McNamara & O'Connell 1989), but much less than is expected from the cooling flow. To explain this Sarazin & O'Connell (1983) made a model predicting that star formation in cooling flows would be biased towards low mass stars, radiating their light predominantly in the near-infrared.

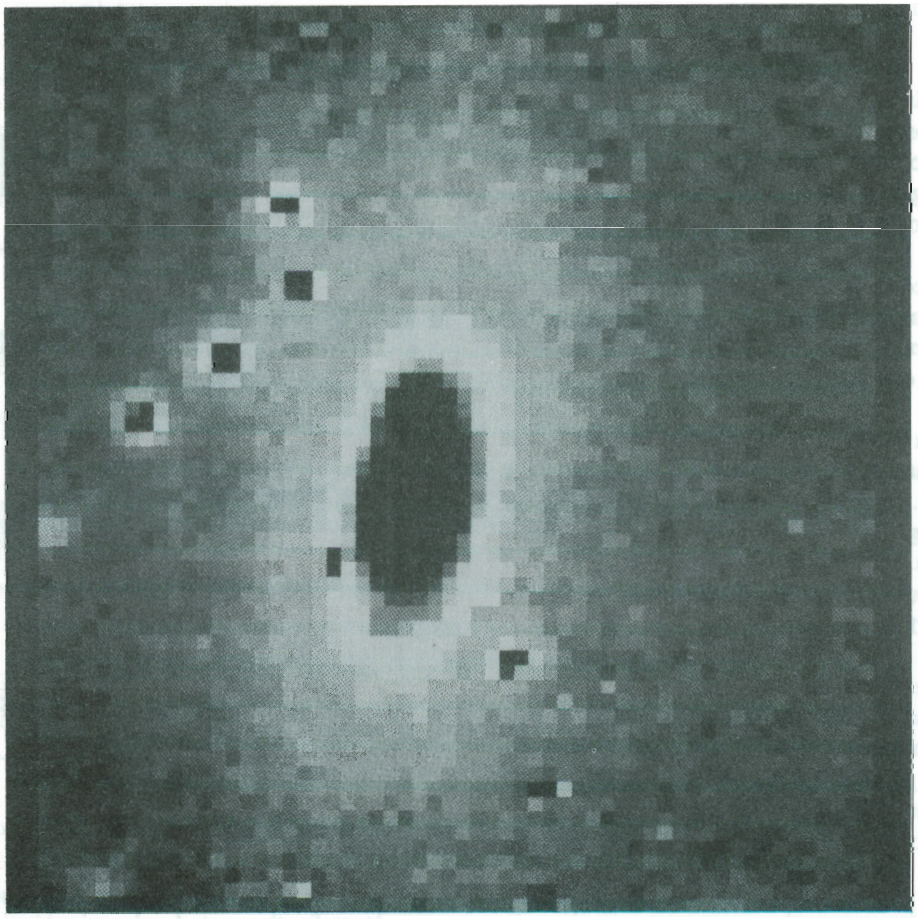

Figure 1. K-image of the central galaxy in Abell 1413. Composite image taken at UKIRT.

In order to test these models we have imaged a sample of 15 galaxies in J and K. The sample consists of galaxies in poor and in rich clusters, with a variety of cooling flows.

The observations were taken with IRCAM at UKIRT and with the 256 x 256 HgCdTe camera of the 2.2m telescope of the University of Hawaii. Because of field and pixel size UKIRT was used to measure the inner regions, while with the UH telescope the outer regions of the galaxies were imaged. Since cDs have an extremely low surface brightness (central values are comparable to disks of spiral galaxies) it was necessary to go very deep, to be able to measure colour gradients in a reliable way. Using a complicated observing procedure we have been able to measure colours at very low surface brightness levels: we obtained an accuracy of 10% at J = 21.7 and K = 20.9 mag arcsec^{-2}. This was done by 'dithering' the galaxy, by moving the image centre around by small amounts on the sky, and in the meantime also offsetting to a sky field approximately 10' away. To reduce the data the frames were sky subtracted, flatfielded and for each galaxy a final mosaic was made.

In Fig. 1 we show some reduced data from IRCAM. In order to obtain colour gradients we fitted ellipses to all frames in infrared and additional optical bands, after having marked by hand the regions of interfering stars and galaxies, so that the program would ignore those. Since we found that isophote shapes were independent of passband, colour profiles could be determined by directly comparing the luminosity profiles in the various bands. We show colour profiles in 7 colours for one galaxy in Fig. 2.

The regions in which the colours are affected by the seeing or undersampling has been indicated by a dashed line. In the outer regions the errors caused by choosing a wrong sky background have been indicated as well. Since the colour profiles showed so little structure, global gradients per decade in radius could be calculated.

The main result of the study is that as far as colours are concerned cDs do not differ from giant ellipticals, neither in their centres nor in their outer parts. The galaxies are seen to become bluer very slowly when going outward, even slightly slower than is the case for gEs. In Fig. 3 we show the R - K gradient as a function of blue luminosity M_B for this sample and the sample of Peletier *et al.* (1990). It shows that the IMF in cDs is likely to be similar everywhere to the one in gEs. Secondly, it supports the hierarchical clustering picture of the formation of cDs (see e.g. Faber *et al.* 1991). In this picture galaxies are made by the merger of smaller galaxies, which all have modest abundance gradients caused by dissipational collapse. The effect of the subsequent mergers is to slowly dilute the existing gradients, predicting that gradients in cDs are not larger than those in giant elliptical galaxies. If the whole galaxy was created by dissipational collapse, and only the halo was formed from tidal debris, the gradient in the old stellar population, as measured in R - K, would be larger than in gEs. The picture is the same in optical colour gradients, except in the very inner regions, which often contain an additional blue stellar population, especially in galaxies with large cooling flows (McNamara & O'Connell 1991). The R - K colour is not very sensitive to young stellar populations, and is mainly an indicator of the old stars.

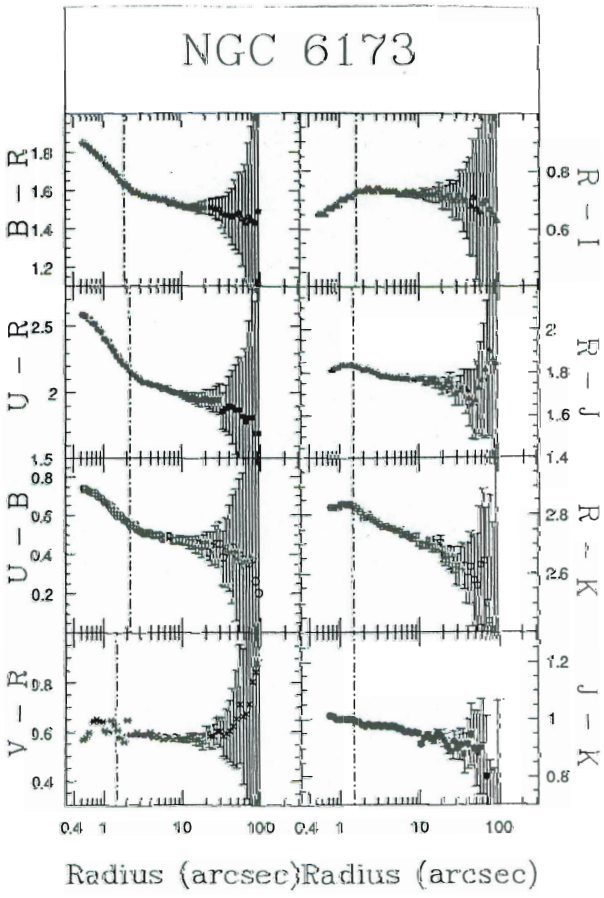

Figure 2. Colour profiles in optical and infrared colours for the central galaxy in Abell 2197.

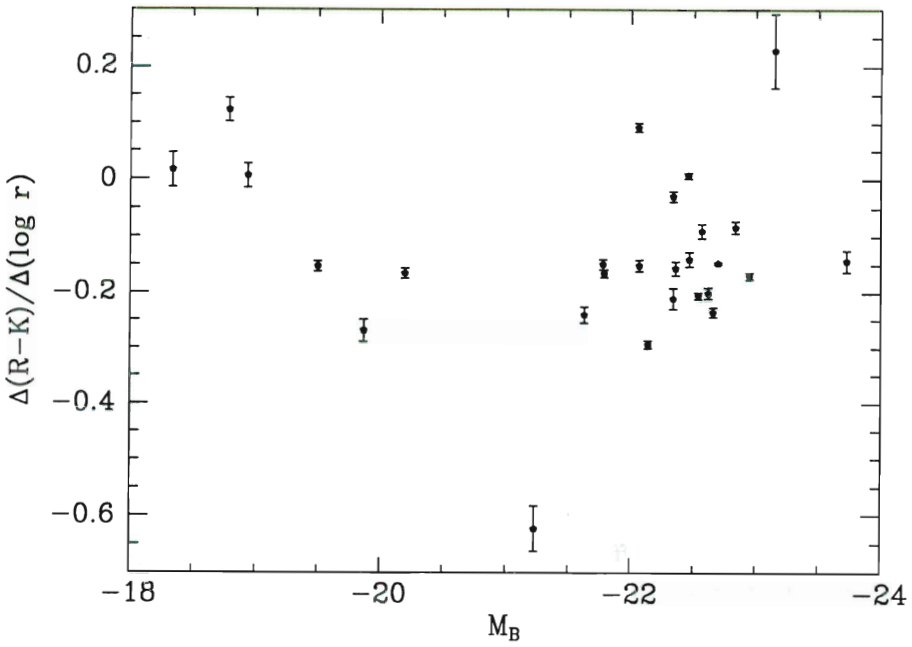

Figure 3. *R - K* colour gradient in mag. per dex as a function of total blue luminosity of the galaxy (with H_o = 75 km s^{-1} Mpc^{-1}) for brightest cluster members and giant ellipticals. Errors are formal errors from a least-squares fit.

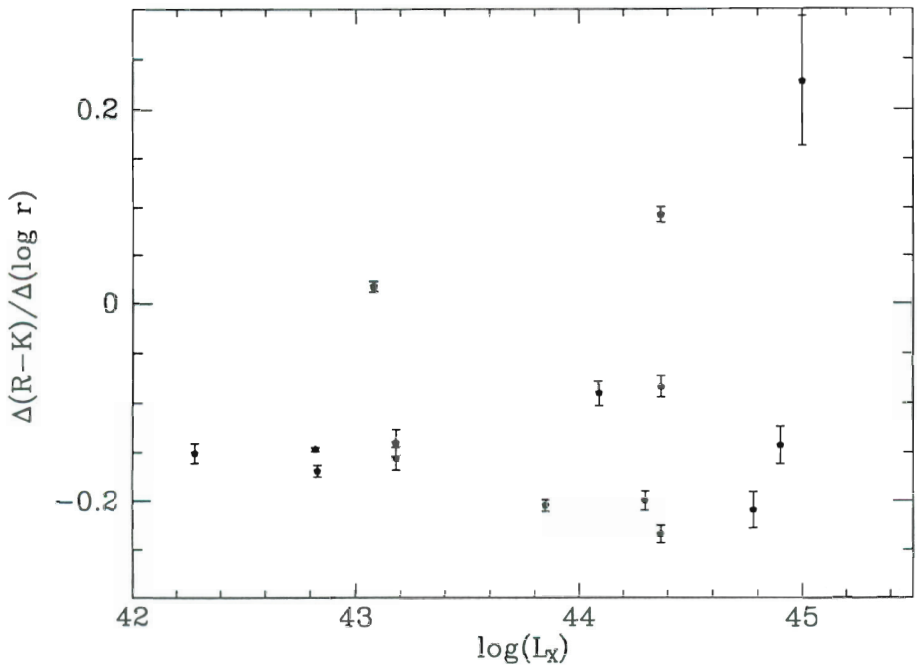

Figure 4. *R - K* colour gradient in mag. per dex as a function of X-ray luminosity of the cluster between 0.5 and 3.0 keV for the sample of brightest cluster members.

In Fig. 4 we have shown the relation of the R - K gradient with total X-ray luminosity between 0.5 and 3.0 keV (from Sarazin 1988). No relations is seen, which means that the cooling flows do not significantly affect the old stellar population of the galaxies. The combination of optical and infrared colours can be used to put constraints on the IMF of the stars forming in the cooling flow (O'Connell & McNamara 1989). In only 2, possibly 3 of the 15 galaxies the outer parts are redder in R - K than in the nucleus, showing that in general we do not see any sign of star formation from cooling flows in the outer regions, and no evidence for red envelopes (Valentijn & Moorwood 1985, McNamara & O'Connell 1991). However it is still possible that the stellar populations in the extended haloes are significantly different. Our photometry unfortunately does not go deep enough to say anything about colours there.

We conclude that colour gradients of cDs are similar or slightly smaller than those in gEs, strengthening the hypothesis that they have been made in mergers of smaller entities. No evidence is found for low mass star formation in cooling flows, with the possible exception of 2 or 3 galaxies.

References

Faber, S.M., Worthey, G. and Gonzales, J.J., 1991, in *The Stellar Populations of Galaxies*, ed. B. Barbuy, IAU 149.

Fabian, A.C. and Nulsen, P.E.J., 1977, *Mon. Not. R. astr. Soc.* **180**, 479.

Gunn, J.E. and Tinsley, B.M., 1976, *Astrophys. J.* **210**, 1.

Hausman, M.A. and Ostriker, J.P., 1978, *Astrophys. J.* **224**, 320.

Malamuth, E.M. and Richstone, D.O., 1984, *Astrophys. j.* **276**, 413.

Matthews, T.A., Morgan, W.W. and Schmidt, M., 1964, *Astrophys. J.* **140**, 35.

McNamara, B. and O'Connell, R., 1989, *Astron. J.* **98**, 2018.

McNamara, B. and O'Connell, R.W., 1991, submitted to the *Astrophysical Journal*.

O'Connell, R.W. and McNamara, B., 1989. *Astron. J.* **98**, 190.

Peletier, R.F., Valentijn, E.A. and Jameson, R.F., *Astron. Astrophys.* **233**, 62.

Sarazin, C.L., 1988, *X-ray emissions from Galaxies*, Cambridge University Press.

Sarazin, C.L. and O'Connell, R.W., 1983, *Astrophys. J.* **268**, 552.

Valentijn, E.A. and Moorwood, A.F.J., 1985, *Astron. Astrophys.* **143**, 46.

R.F. Peletier
European Southern Observatory
Garching, and
Center of Astrophysics
Cambridge
Mass. USA

D. Carter
Royal Greenwich Observatory
Cambridge, UK

D. Mackie
Department of Astronomy
University of Wisconsin
Madison, USA

A.J. Pickles
IfA
University of Hawaii, USA

N. Visvanathan
Mount Stromlo and Siding Springs Observatory
Australia

A Set of Faint JHK Standards for UKIRT

Why do we need Faint IR Standard Stars?

The introduction of sensitive array detectors for IR imaging has meant that sources as faint as K=17-20 are now regularly imaged with UKIRT and other 4m class telescopes. A large gap has therefore emerged between the magnitudes of target objects and the stars which have traditionally been used as standards in the near IR. For example, the Elias list of bright standards has K=3-4, while Elias `faint´ standards have a K of around 7 or 10,000 times brighter than the objects frequently imaged. With such a range of brightness one needs to be very confident of understanding detector peculiarities such as non-linearity, if an accurate calibration is to be achieved. Of further concern is the fact that bright standards can only be imaged with exposures much shorter than those typically used to achieve background limited performance on faint objects.

Although magnitude checks since 1989 have shown that there are no serious systematic errors in IRCAM photometry of faint objects, it was decided that to ensure good photometry in the future, a program to measure a set of faint standards (K > 12) for UKIRT should be conducted, and to this end PATT time was awarded over two semesters.

Observations

Observations were made over 17 separate nights consisting of both whole and half nights. A total of 36 faint stars, selected from the lists by Landolt (1983) and from the HST photometric standards (Turnshek *et al.* 1990) were observed at JHK with the single channel photometer UKT9 which has traditionally defined the UKIRT system. The goal was to observe each star a few times each night and to repeat this on at least 3 separate nights. This was achieved for all but a handful of objects. The existing UKIRT bright standards (3 < K < 7) were also observed frequently to provide the calibration.

The Bright Standards

The first step in reduction was to check the UKIRT bright standards for consistency. The majority of these stars are from the list of Elias (1982), with magnitudes modified over the years so that they effectively defined a UKIRT system. Our observations revealed that while the mean zeropoint of the bright standards was quite consistent and well defined for A0 stars, there existed a small colour dependent error which for red stars (J - K = 1) amounted to 3% in the worst case for L´ and H. The first step in reduction was therefore to correct the bright standards for this effect. The new default bright standard magnitudes at the telescope have been updated with this correction.

The Faint Standards

The new faint standard (8 < K < 15) magnitudes are determined to better than 3% for 33 of the final list of 34 stars with about half the sample better than 1% precision as determined from the scatter in magnitudes obtained on different nights. Results are shown in the table below with the formal RMS

Faint Standards Cross Reference

Name	Ref	Name	Ref	Name	Ref
FS 1 G158-100	2	FS 12 GD71	1	FS 24 SA106-1024	1
2 SA92-342	1	13 SA97-249	1	25 SA107-1006	1
3 F11	1,2	14 Rubin 149	2	26 SA108-475	1
4 SA93-317	1	15 M67-I-48	3	27 M13-A14	4
5 F16	1,2	16 M67-IV-8	3	28 SA109-71	1
6 F22	1,2	17 M67-IV-27	3	29 G93-48	1,2
7 SA94-242	1	18 SA100-280	1	30 SA114-750	1
8 SA94-251	1	19 G162-66	1,2	31 GD246	1,2
9 SA94-702	1	20 G163-50	1,2	32 F108	1,2
10 GD50	2	21 GD140	4	33 GD153	4
11 SA96-83	1	23 M3-193	4	34 EG141	4
				35 G21-15	2

TABLE OF FAINT STANDARDS

Name	RA (1950)	Dec (1950)	K	J-K	H-K
FS 1	00 31 22.7	-12 24 29	12.967 (0.021)	0.462 (0.011)	0.081 (0.012)
FS 2	00 52 36.0	00 26 58	10.466 (0.003)	0.247 (0.003)	0.038 (0.003)
FS 3	01 01 46.6	03 57 34	12.822 (0.007)	-0.222 (0.011)	-0.097 (0.007)
FS 4	01 52 03.7	00 28 20	10.264 (0.005)	0.292 (0.003)	0.040 (0.007)
FS 5	01 52 04.7	-07 00 47	12.342 (0.006)	-0.007 (0.004)	-0.002 (0.004)
FS 6	02 27 39.2	05 02 34	13.374 (0.015)	-0.135 (0.014)	-0.069 (0.012)
FS 7	02 54 47.2	00 06 39	10.940 (0.005)	0.165 (0.012)	0.037 (0.010)
FS 8	02 55 12.9	00 04 04	8.313 (0.006)	0.766 (0.002)	0.129 (0.004)
FS 9	02 55 38.8	00 58 54	8.266 (0.006)	0.884 (0.003)	0.158 (0.005)
FS 10	03 46 17.4	-01 07 38	14.919 (0.072)	-0.170 (0.077)	-0.049 (0.060)
FS 11	04 50 25.4	-00 19 34	11.278 (0.018)	0.076 (0.025)	0.016 (0.019)
FS 12	05 49 34.8	15 52 37	13.898 (0.003)	-0.217 (0.014)	-0.091 (0.018)
FS 13	05 54 33.8	00 00 53	10.135 (0.003)	0.382 (0.002)	0.047 (0.005)
FS 14	07 21 41.2	-00 27 10	14.261 (0.012)	-0.153 (0.005)	-0.079 (0.020)
FS 15	08 48 21.9	11 55 02	12.360 (0.021)	0.418 (0.008)	0.060 (0.007)
FS 16	08 48 31.0	12 00 36	12.631 (0.008)	0.340 (0.006)	0.038 (0.005)
FS 17	08 48 35.4	12 03 26	12.270 (0.007)	0.411 (0.007)	0.073 (0.003)
FS 18	08 51 02.1	-00 25 14	10.522 (0.008)	0.292 (0.003)	0.031 (0.003)
FS 19	10 31 14.5	-11 26 08	13.796 (0.025)	-0.231 (0.021)	-0.142 (0.047)
FS 20	11 05 27.6	-04 53 04	13.473 (0.017)	-0.120 (0.015)	-0.069 (0.012)
FS 21	11 34 27.6	30 04 35	13.132 (0.004)	-0.184 (0.033)	-0.101 (0.037)
FS 33	12 54 35.1	22 18 08	14.240 (0.016)	-0.223 (0.010)	-0.078 (0.024)
FS 23	13 39 25.7	28 44 59	12.374 (0.000)	0.623 (0.004)	0.072 (0.018)
FS 24	14 37 33.3	00 14 36	10.753 (0.008)	0.151 (0.006)	0.019 (0.004)
FS 25	15 35 59.9	00 24 03	9.756 (0.017)	0.475 (0.003)	0.070 (0.005)
FS 26	16 34 26.3	-00 28 39	7.972 (0.009)	0.858 (0.004)	0.155 (0.006)
FS 27	16 38 54.2	36 26 56	13.123 (0.018)	0.371 (0.013)	0.058 (0.014)
FS 28	17 41 32.5	-00 23 44	10.597 (0.016)	0.148 (0.010)	0.047 (0.005)
FS 35	18 24 44.5	04 01 17	11.757 (0.017)	0.474 (0.008)	0.089 (0.005)
FS 34	20 39 41.9	-20 15 21	12.989 (0.011)	-0.170 (0.008)	-0.070 (0.009)
FS 29	21 49 53.0	02 09 16	13.346 (0.024)	-0.171 (0.011)	-0.075 (0.012)
FS 30	22 39 11.3	00 56 55	12.015 (0.020)	-0.092 (0.013)	-0.036 (0.005)
FS 31	23 09 50.4	10 30 46	14.039 (0.010)	-0.241 (0.020)	-0.120 (0.017)
FS 32	23 13 38.2	-02 06 58	13.664 (0.012)	-0.205 (0.011)	-0.088 (0.015)

errors in parentheses. Colour measurements are significantly better than individual filter measurements, indicating the presence of night to night systematic errors of a few % in the photometry. It should also be noted that a few stars (FS1, 10, 19) need further measurements to bring the errors within acceptable limits.

Magnitudes are presented on the UKIRT natural system. The transformations to the Caltech (CIT) system were re-determined from the many bright standards common to both, and were found to be as follows:

Kcit	=	Kukirt - 0.018 * (J-K)
(J-K)cit	=	0.936 (J-K)ukirt
(H-K)cit	=	0.960 (H-K)ukirt
(J-H)cit	=	0.920 (J-H)ukirt
(K-L)cit	=	0.820 (K-L)ukirt

Results to date (Guarnieri *et al.* 1991) indicate that any differences between UKT9 and IRCAM photometry are less than 2% for stars with J - K < 1. We plan to observe a number of very red objects on the same night with both IRCAM and UKT9 to determine this transformation accurately.

References

[1] Landolt, 1983. A.J. **88**, 439
[2] Turnshek *et al.*, 1990. A.J. **99**, 1243
[3] Eggen and Sandage. Ap.J. **140**, 130
[4] Zuckerman. Private Communication
[5] Elias *et al.*, 1982. A.J. **87**, 1029
[6] Guarnieri *et al.*, 1991. PASP **103**, 675

Mark Casali
Tim Hawarden
JAC, Hawaii
Royal Observatory, Edinburgh

Discovery of a Curving H_2 Jet with Bow-Shocks

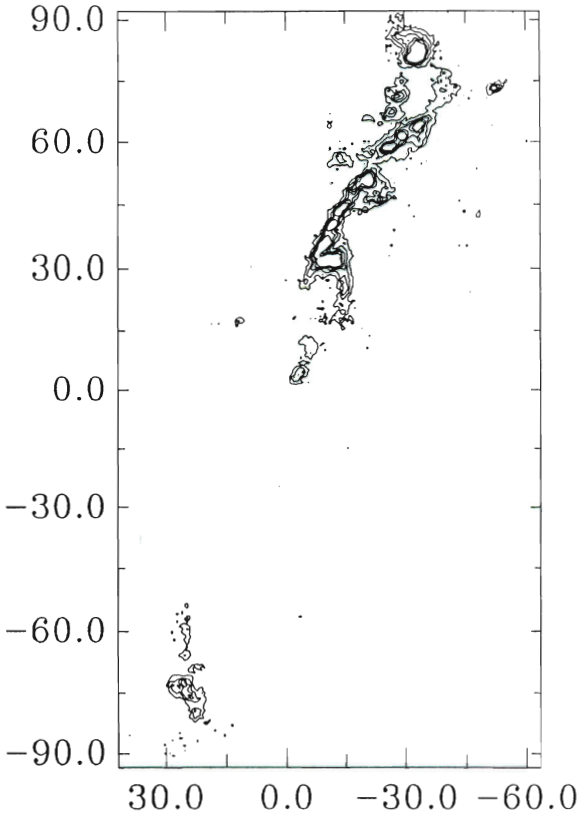

High-resolution (0.6"/pixel) narrow-band IRCAM imaging in the v=1-0 S(1) line of H_2 has revealed a remarkable jet-like structure associated with the high-velocity CO outflow in L1448. The H_2 jet closely follows the curving inner edge of the blue-shifted CO lobe, and seems to represent the shock interface between a neutral stellar wind from the outflow source and the molecular surroundings. Entrainment at this interface probably produces the associated CO outflow.

The jet itself consists of a series of extended knots, together with three bow-shocks equally spaced along the jet length. These bow-shocks may result from individual dense clumps or bullets within the outflow, or from a variable wind ejection rate. Notably, the bow-shock sizes decrease with increasing distance from the source; this trend is consistent with the observed deceleration along the CO outflow.

Chris Davies, Bill Dent, John Lightfoot, Colin Aspin and Henry Matthews
ROE and JACH

Lensed Galaxies at High Redshift: the Infrared Approach

Introduction

The most observationally useful feature of gravitational lensing occurs when the potential well of a foreground cluster of galaxies magnifies and distorts the image of background galaxy into a *giant arc*. This provides an easily identifiable signature which may be used to preferentially select objects at high redshift. Since the lensing process conserves surface brightness, the resulting magnification enables information to be gathered about the dynamics and spectral properties of a distant source on spatial scales normally unattainable. To the limit of spectroscopy with 4-m class telescopes ($b_J \sim 23$-24), magnitude-limited redshift surveys only reach a median depth of $\langle z \rangle \sim 0.3$ and few galaxies are found with $z > 0.7$ (Colless *et al.* 1990, 1992, Cowie *et al.* 1991). Since lensed sources *must* be at reasonable high redshift, even a small sample of such objects will be useful and will complement data on field galaxies derived from such surveys. Most of the arcs with available spectroscopy seem to have blue optical colours, indicative of strong star formation, similar to the *flat spectrum* galaxies that dominate the faint field population (Fort 1990, Mellier *et al.* 1991). If this is correct, a careful study of a few arcs would throw valuable light on the origin of this puzzling population. We have recently carried out such a study, and the results will appear in Smail *et al.* (1992). A summary is presented here.

When observing high redshift galaxies, the three most useful parameters to measure are the mass, the current star formation rate and a time-averaged star formation rate. A comparison of the latter two parameters gives some indication of whether we are witnessing the source in an important phase of its lifetime e.g. during a major episode of star formation. Our approach here will be to examine the colours of the most reliable giant arcs across a wide wavelength range, extending Mellier *et al*'s study to infrared wavelengths. In particular, the combination of optical *and* infrared colours allows us to probe the ratio of present to past star formation, while the infrared luminosity is directly related to the mass of the galaxy. Using these results we address the question of whether the current optically-discovered sample is likely to be representative of high redshift field galaxies in general and to link our observational results with those found from the field redshift surveys.

The Need for Infrared Data

It is well known that star forming galaxies become more readily visible at modest redshifts when surveyed in optical bands than those dominated by old stellar populations. This selection bias occurs because the rest-frame ultraviolet (dominated by light from hot young stars) is redshifted into the observing passband. Although the blue colour of many of the arcs discussed in Meiller *et al.* indicate sources with strong star formation, the implications for galaxy evolution are unclear. The critical question is whether we are witnessing a low mass dwarf made temporarily luminous by a burst of star formation, a massive system whose bulk star formation was much higher in the past, or a normal late-type galaxy with a moderate but continuous star formation rate. For example, a massive spiral galaxy with continuous star formation would appear similar, in terms of its rest-frame ultraviolet spectral energy distribution, to a less massive galaxy undergoing a more intense, but short-lived, burst of star formation. Optical data alone cannot readily disentangle these very different scenarios. An optical-infrared colour such as $R - K$, combined with an optical colour such as $B - R$ allows a ready discrimination between the two cases above, primarily because it is sensitive to any underlying evolved stellar population. Therefore, to obtain a representative view of the stellar populations of the distant arc sample, it is thus essential to add photometry from near-infrared bands. Furthermore, if the lensing magnification can be understood, infrared photometry provides a robust estimate of the mass in stars of the system, since it is sensitive to light from long-lived stars that dominate the stellar mass function.

The Data

Our sample consists of the 7 available giant arcs with either genuine redshifts or redshift constraints from spectral information. Our strategy has been to measure 2μm K band photometry and combine it with optical CCD photometry in B and R.

The new infrared data consists of very deep K band images obtained on UKIRT using IRCAM in both 0.62 and 1.24 arcsec pixel^{-1} scales. In general, the smaller pixel scale is better matched to the seeing, allowing more accurate photometry in the crowded cluster environments. However, the field of view is then restricted especially when using in-field

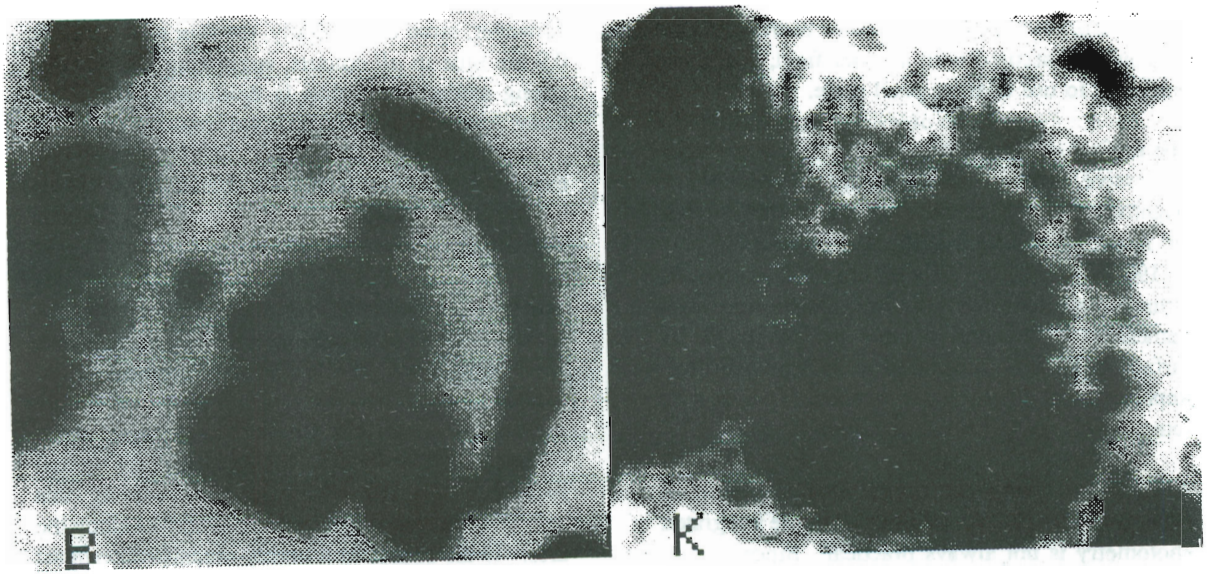

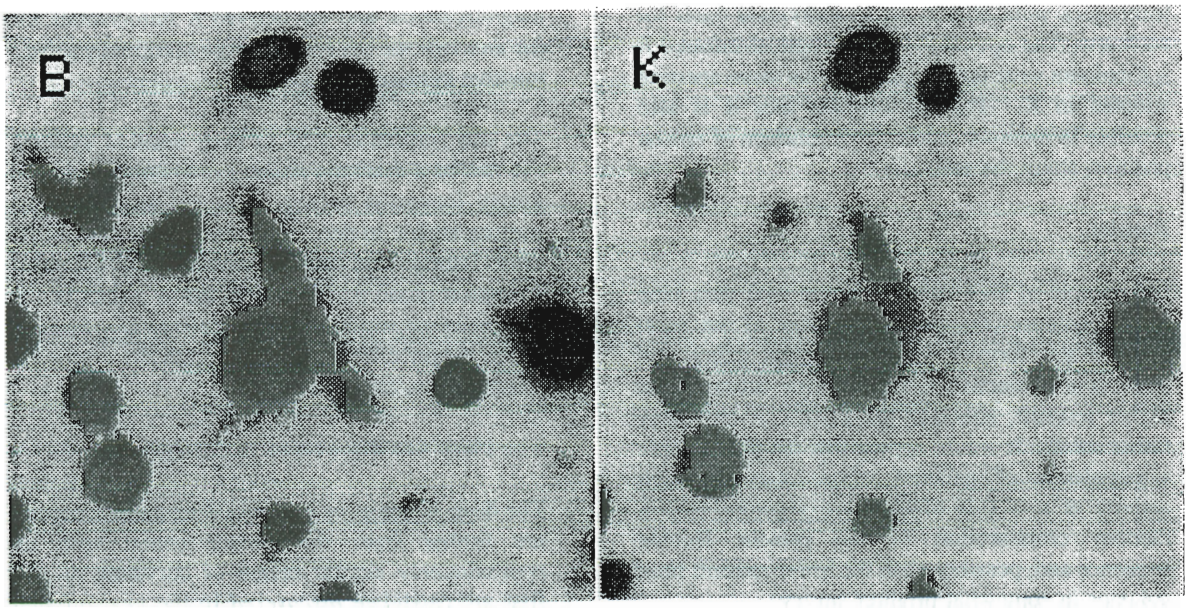

Figure 1. Broad band images of selected arcs in our sample. North is at the top, East is at the left. **Top:** *B* and *K* images of C12244-02, the giant arc is clearly detected in the *K* image. The second infrared arc is concentric with the giant arc and North-West of it. The vast difference in the arcs' colours can be seen by comparing the *B* and *K* images. The frames are 25 arcsec square. **Bottom:** *B* and *K* images of Abell 2390. The images are 29 x 27 arcsec. The strong colour gradient along the arc is obvious.

dithering methods to flatfield the data to the required precision for detecting the low surface brightness arcs against the bright sky in K (*cf.* Cowie *et al.* 1988). In some cases more than one arc could be secured with a wider field, making it profitable to use a larger pixel scale.

The in-field dithering technique produces the most impressive results, penetrating to fainter surface brightness limits than those quoted in earlier work (*cf.* Aragón-Salamanca 1991, Aragón-Salamanca *et al.* 1992). In a 3.3 hrs dithered exposure, we obtain virtually photon-noise limited performance, a flatness of better than 4 parts in 10^5 and a 1σ surface brightness limit of $\mu_K = 23.5$ mag/arcsec^2. Representative K images are reproduced along with some optical CCD frames in Figure 1.

Since the arcs are often irregular or embedded in the envelopes of cluster ellipticals precise integrated photometry is not always practical. Since we are principally interested in colours, we chose to measure within fixed apertures. To standardize across the optical and infrared, the optical frames were resampled onto the infrared pixel scale, rotated and aligned. Images were also smoothed when there was significant differences in the seeing conditions amongst the various filters. This latter step produces only a small correction to the actual colours. Aperture sizes and background subtraction techniques were chosen on an individual basis for each arc. The optical $B - R$ and optical-infrared $R - K$ colours were measured using the same aperture adopted in K. For the brighter arcs it is also possible to measure colours as a function of spatial position along the arc.

Results

Our sample of arcs include objects with very blue optical colours ($B - R \leq 1$) typical of the most extreme star forming galaxies present today, and there is a distinctive trend to bluer colours with higher redshift, although the sample is obviously rather small. It would appear that the arcs sample a population of galaxies whose star formation activity at $z \sim 1$ is much more vigorous than a random cross-section of the present Hubble sequence and, possibly, than the lower redshift field galaxies in somewhat brighter surveys.

But optical colours can mislead at high redshift because of biases introduced by ultraviolet flux which enters the optical region. Indeed, several of the arcs with $z < 1$ which are blue in $B - R$ turn out to have fairly reasonable colours in $R - K$ indicative of precisely this effect. Only a small amount of additional star formation in a normal spiral would be needed to explain the combined BRK colours. However, more interestingly, the four arcs with $z > 0.9$ are blue in *all* colours, suggesting a genuinely young stellar population is dominating the light. They have no significant contributions from an evolved population and cannot, therefore, readily be explained via subsidiary star bursts of a minor nature superimposed on a pre-existing stellar population.

The gravitational magnification for the arcs in our sample is an issue central to resolving the question of whether we are witnessing vigorous star formation in massive ($\sim L^*$) systems or simply seeing individual star forming clumps, either in isolation, or star forming portions of fairly normal systems. An approach towards resolving this ambiguity is to search for colour gradients along the arcs. If the source is a highly-magnified compact HII region, taking an extreme example, one might expect a remarkably uniform colour, whereas a more massive system might show a variation in colour representative of resolved portions each exhibiting different star formation rates. Such gradients have been measured in two arcs Abell 2390 and Cl2244-02 (Figure 1). The existence of gradients, together with other arguments (see Smail *et al.* 1992 for details) point towards moderate magnifications, and the derived K luminosities for the arcs indicate the sources to be marginally sub-L^* massive systems.

The star formation seen in such massive systems can not be a dramatic single event associated with galaxy formation because it would render typical sources visible in deep spectroscopic field surveys. More likely, we are witnessing an extended formation phase which culminates at redshifts $\sim$1. If correct, we would not expect to see any features in the galaxy counts associated with the primaeval phase to $B \sim 26$.

The First Arc discovered in the Infrared

The deep K image of Cl2244-02 revealed a second arc further from the cluster centre with an approximately similar centre of curvature — the first arc candidate *discovered* in the near-infrared (see Figure 1). Its detection prompted the acquisition of a much deeper B image which shows the second arc at a surface brightness of μ_B=27.6 mag/arcsec^2. In the deep high resolution B data, the second arc is approximately 10 arcsec long and appears unresolved. In contrast to the main sample,

although this arc appears blue in the optical ($B - R \leq 1$), it is prominent in K and hence very red in the optical-infrared region ($B - K = 7.3$ and $R - K \geq 6.3$). An early-type galaxy placed at the cluster's redshift ($z = 0.329$) had $B - K \sim 6.2$ and reaches $B - K = 7.3$ at $z \sim 0.6$, when $R - K = 4.3$. However, the unusual feature of the arc is the faintness in R — the limits given by this in $R - K$ require the source to have $z \geq 1.2$ and the $B - R$ value then needs a strong upturn in the SED below 2000Å. However, it is sufficiently faint, especially in the optical, that these colours must be viewed with some caution.

A simple geometric lensing model suggests the second arc should be at least as distant as the primary arc, and more likely at an even greater distance. The colours are consistent to those expected for an E/S0-Sab with a strong UV upturn observed at the redshift of the giant arc; in this case the source would be luminous with $M_K \sim -25.7$. Its optical detection suggests the Lyman limit has not reached the B band and thus $z < 3.8$. The red optical-infrared colour is important, however, in view of the near uniform optical-infrared colours for the optically-selected arcs. It suggests there might be very strong selection effects operating in the identification of arcs.

Concluding Remarks

When studying the formation of galaxies, and in particular L^* galaxies, the crucial observational domain is $1 < z < 2$. Gravitational lensing is an ideal tool to probe this region. When combined with infrared observations, it allows us an unbiased view of galaxies during this important period in their histories. The observations presented here imply that we are witnessing an extended era of star formation in the arc sources — possibly associated with the disk formation in the L^* field galaxy population.

References

Aragón-Salamanca, A., 1991, PhD Thesis, Durham University.

Aragón-Salamanca, A., Ellis, R.S., Schwartzenberg, J-M. and Bergeron, J., 1992, *in preparation*.

Colless, M.M., Ellis, R.S., Taylor, K. and Hook, R.N., 1990, *Mon. Not. R. astr. Soc.*, **244**, 408.

Colless, M.M., Ellis, R.S., Broadhurst, T.J., Taylor, K. and Peterson, B.A., 1992, *Mon. Not. R. astr. Soc.*, submitted.

Cowie, L.L., Lilly, S.J., Gardner, J.P. and McLean, I.S., 1988, *Astrophys. J.*, **332**, L29.

Cowie, L.L. Songaila, A. and Hu, E.M., 1991, *Nature*, **354**, 460.

Fort, B., 1990, In *Gravitational Lensing*, eds. Mellier, Y., Soucail, G., Fort, B., Springer-Verlag, p221.

Mellier, Y., Fort, B., Soucail, G., Mathez, G. and Cailloux, M., 1991, *Astron. Astrophys.*, **380**, 334.

Smail, I., Ellis, R.S., Aragón-Salamanca, A., Soucail, G., Mellier, Y. and Giraud, E., 1992, *Mon. Not. R. astr. Soc.*, submitted.

Alfonso Aragón-Salamanca
Ian Smail
Richard Ellis
Physics Department
University of Durham

JCMT Observations of DR21(OH)

DR21(OH) is a dense star formation region situated about 3 arc minutes North of the HII region and molecular cloud DR21. It appears more quiescent than its Southern neighbour, and is thought to represent an earlier stage in the star formation process. Recent observations (Richardson, Sandell and Krisciunas 1989, Mangum *et al.* 1991, 1992) have shown it to have a multiple peaked structure and it has been identified as a massive protocluster. It is dense and highly obscured, and observations in high-density tracers such as CS, and the relatively optically thin millimetre and submillimetre continuum, provide a good way of revealing its structure.

Such observations have been made on the JCMT. The source was mapped in the J=5-4 transition of CS, using the Kent/RAL testbed receiver (see Protostar Issue No. 8), with some additional observations made with Receiver A. Several lines of methanol, detected in the image sideband of the SIS Receiver, were also mapped. At a later date, the region was mapped in the continuum at 450, 800 and 1100 microns with UKT14. The line

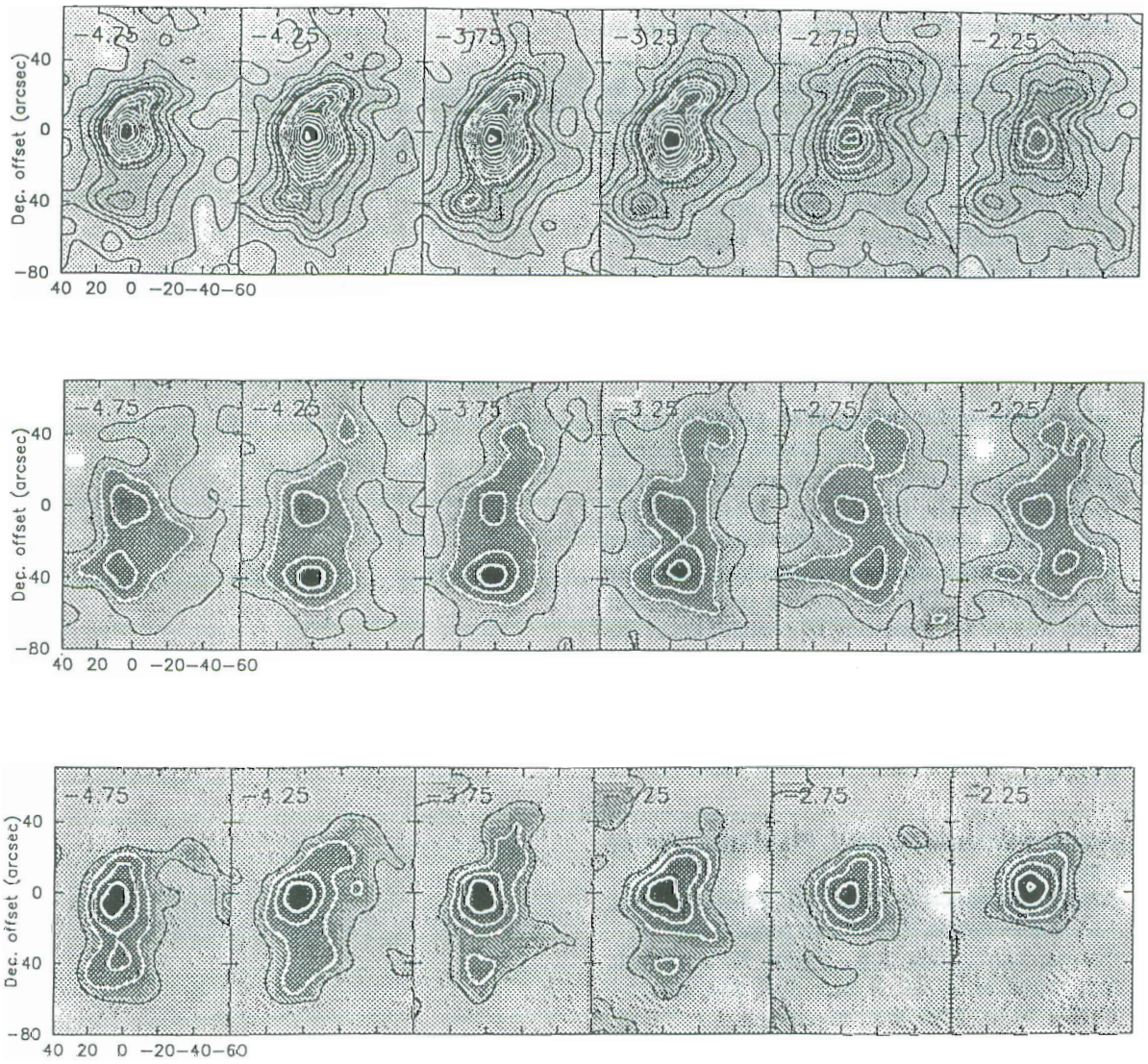

Figure 1. Channel maps, in 0.5 km/s velocity channels, central part of the line, in transitions CS J = 5 - 4 (top), CH_3OH 5(0) - 4(0) A+ (middle) and CH_3OH 5(1) - 4(1) E1/E2 (bottom).

observations were reduced with SPECX; and the continuum observations initially with NOD2, followed by deconvolution using the newly available DBMEM maximum entropy software.

Examples of the line observations are shown in Figure 1. Channel maps across the line centre are shown in 0.5 km/s velocity channels for the transitions (from top to bottom) CS J=5-4, CH_3OH 5(0)-4(0) A+, and CH_3OH 5(2)-4(2) (blend of E1 and E2). Continuum maps at 800 and 450 microns are also shown, in Figures 2 and 3.

The central source, DR21(OH) (main), shows up strongly in all maps. At 450 microns, where our spatial resolution was highest (8 arc sec FWHM), the source appears elongated NE-SW, and in fact interferometric observations (Mangum *et al.* 1992) have shown that two sources (MM1 and MM2) are present, which our 450 micron map does not quite resolve. However, the 450 micron emission does appear to peak around the position of the hotter MM1 source to the NE.

On the CS spectrum towards DR21(OH)(main), we observe low-intensity, high velocity wings, extending over about 80 km/s (Figure 4). Emission over such a high velocity range has not been observed before towards this source. It is probably due to a young, compact outflow.

In all maps, line and continuum, we see emission around 40 arc sec to the South of DR21(OH)(main). Its structure is relatively complex and varies between maps, probably because of a combination of temperature, density and abundance gradients. In the line maps, it is possible to discern three separate sources having different lsr velocities; DR21(OH)SW (~ -2 km/s), DR21(OH)S (~ -4.2 km/s), and DR21(OH)SE (~ -3.2 km/s). In the CS map, only the SE source is particularly strong, probably because the S and SW sources are not hot enough (though they are almost certainly dense enough) to fully excite this transition. Of the lines observed, the one with the lowest energy levels is CH_3OH 5(0)-4(0) A+ [E(lower)=23K] and it is in this line that the S and SW sources show up particularly strongly; indeed the S source is even stronger than DR21(OH)(main).

The present observations indicate that methanol is as abundant, if not more so in the Southern sources compared with the main source, which suggests that methanol production can be explained by gas phase models which take account of depletion onto and evaporation from grain surfaces (e.g. Brown *et al.* 1988).

DR21(OH)(main) bears some similarity to the Southern molecular peak in OMC-1, which shows wings in SO but not particularly in CO. The Southern sources are colder and, apparently, more

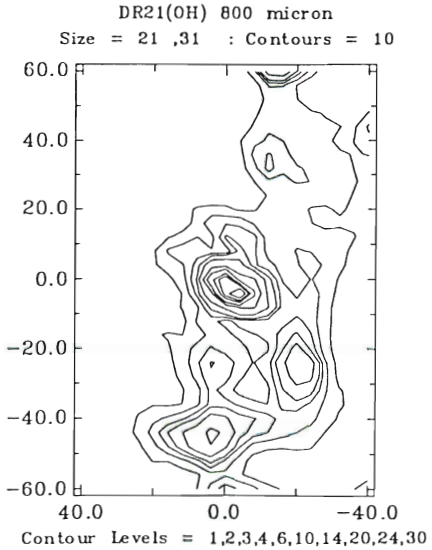

Figure 2. DR21(OH) in the 800 micron continuum. Contour levels are in units of 10^8 Jy/sr.

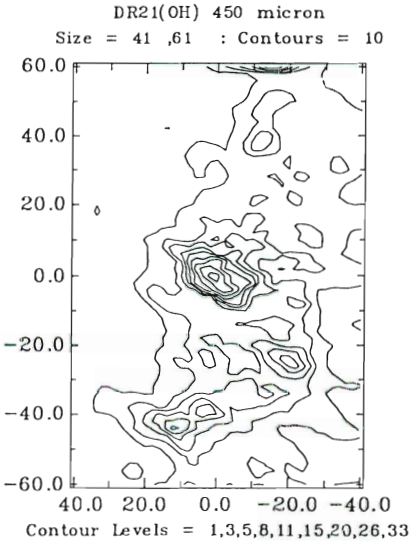

Figure 3. DR21(OH) in the 450 micron continuum. Contours in units of 10^8 Jy/sr.

quiescent, and they perhaps represent an even earlier stage in the star formation process, before disruptive events such as outflows have started.

Collaborations

Also involved in this project are Charles Cunningham (HIA), Steve Davies (UKC), Matt Griffin (QMW), John Richer (MRAO) and Göran Sandell (JACH).

References

Mangum, J.G., Wootten, A., Mundy, L.G., 1991, *ApJ.* **378**, 576.
Mangum, J.G., Wootten, A., Mundy, L.G., 1992, *ApJ.* **388**, 477.
Richardson, K.J., Sandell, G., Krisciunas, K., 1989, *Astron. Astrophys.* **224**, 199.

K.J. Richardson
Queen Mary and Westfield College
London

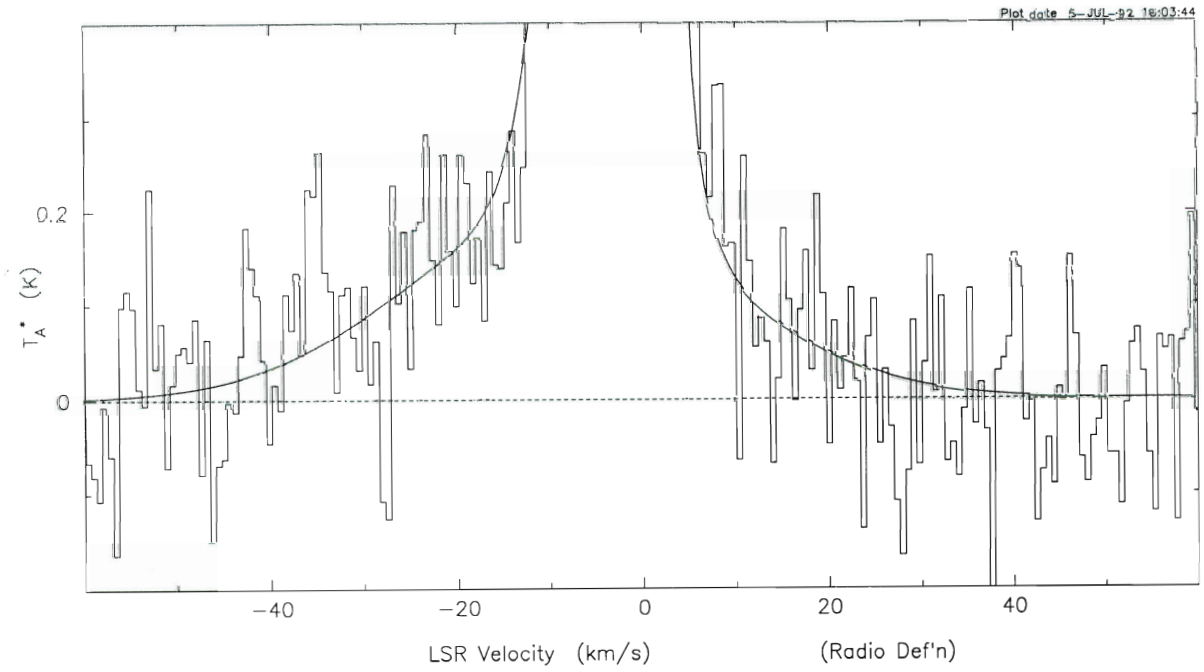

Scan 14 0042.001 dr21oh JCMT Obs'd 22-MAY-89 at 13:29:11(UT)
Map centre: 20 37 13.98; 42 12 09.98 Offset(R,D): (0 0) arcsec
Int'n time: 2550.00 sec; Elevation: 60.7 deg; Vlsr: −20.0 Km/s

Quad.	#pts.	Cent.Ch	Rest Freq(GHz)	Obs.Freq(GHz)	Inc.freq(MHz)	Tsys(K)
1	1024	512.5	244.9357	244.9386	0.497	837.99

Figure 4. The high velocity wings towards DR21(OH) (0,0), observed in the CS J = 5 - 4 transition.

Polarimetry of High-Mass and Low-Mass Star-Formation Regions

We report JCMT observations made with UKT14 and the Aberdeen/QMW Polarimeter, in November 1991 and March 1992. The aim of the project was to compare the magnetic field morphology (via polarised emission from partially-aligned grains) in cloud cores containing low-mass and high-mass YSOs. Theories such as those of Shu and collaborators suggest that high-mass stars form when too much mass is present to be supported by the magnetic field, resulting in sudden collapse, whereas low-mass stars form when the field gradually diffuses out of the cloud by ambipolar diffusion (ion-neutral drag). In the former case, the magnetic field lines are expected to be very 'pinched-in' at the YSO position, while in the latter they will be much less bent.

These models are often accepted as correct, although in fact there is very little observational evidence on magnetic fields in molecular clouds. The installation of the new polarimeter on the JCMT provided a first opportunity to test the models, by measuring the degree of alignment of the grains in the cloud core.

Our preliminary results are shown below (Figs.1 and 2), for the sources W3 IRS5 and Rho Oph SM1 (high-mass and low-mass objects respectively). The vectors show the direction of the polarisation, which is parallel to the grain long axes (i.e. perpendicular to the magnetic field). The length of the vectors is proportional to the percentage polarisation, and the polarisation angle is measured anticlockwise from the vertical. The polarisation percentages are typically 4 sigma detections, and the errors on the angles are approximately +/-10 degrees. The polarisation data is overlaid on maps of the sources at the same wavelength (800 microns), obtained by

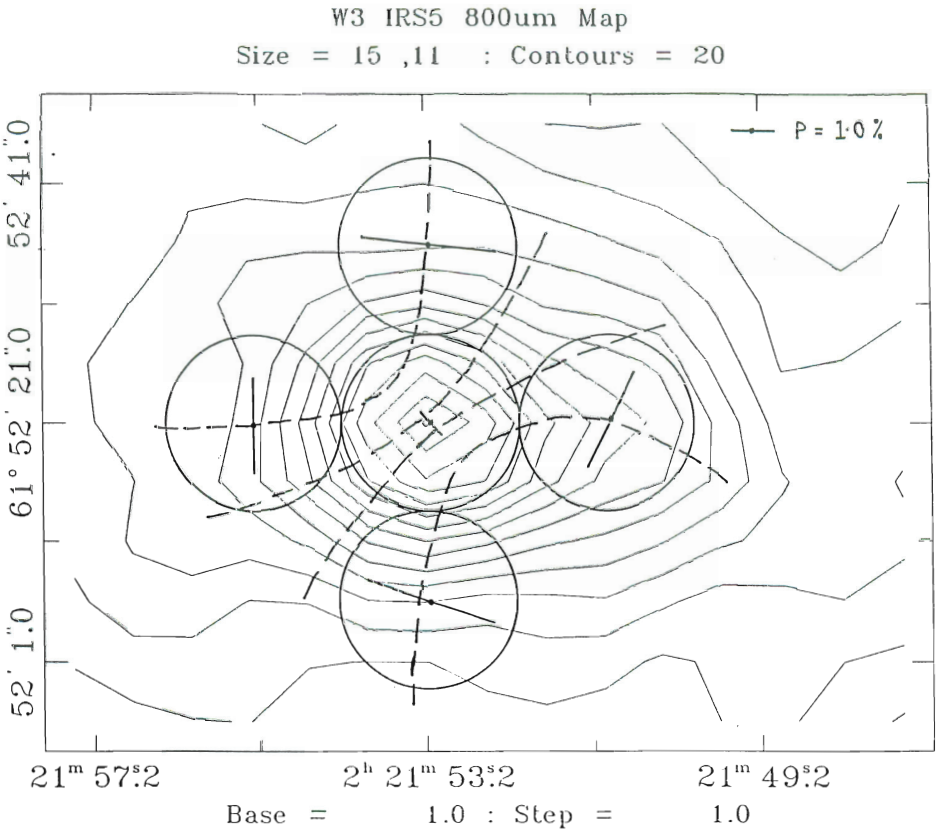

Figure 1. 800 micron map of W3 IRS5, overlaid with 800 micron polarisation vectors. Co-ordinates are R.A.(1950) and Dec.(1950). The circles indicate the diffraction-limited beam FWHM, and a 1 percent polarisation vector is shown for scaling purposes. The dashed lines indicate suggested magnetic field lines.

us (Rho Oph SM1) and by Oldham, Richardson, Griffin and Sandell (W3 region, 1992, in preparation).

We have sketched in possible magnetic field morphologies, and find that these ARE consistent with our expectations. Thus the models for star-formation via supercritical collapse or ambipolar diffusion may well be correct, although more sources need to be observed to confirm this.

Much of the data reduction was done at the telescope, using online packages which fit sine and cosine functions to the plot of flux versus position angle of the polarimeter waveplate (see the Observer's Guide and the report by Murray in the JCMT/UKIRT Newsletter of August 1991). We then subtracted off the polarisation due to the instrument (IP). Observations made in November and March using Jupiter (assumed to be an unpolarised source), indicated that the IP was 0.5 percent at 800 microns on both occasions. Finally, the scans for each position were averaged, and the polarisation percentage and direction were obtained from the corrected amplitudes of the sine and cosine functions. Each vector shown is the result of averaging 3 - 7 scans, each of 20 minutes duration.

A more detailed description will be given in the final publication, which will include a few other positions observed in W3 IRS4, W3(OH) and Mon R2. We wish to thank the telescope staff for their help, especially Goeran Sandell and Bill Duncan.

Jane Greaves, Wayne Holland, Sye Murray and Graeme Oldham
Queen Mary and Westfield College (University of London)

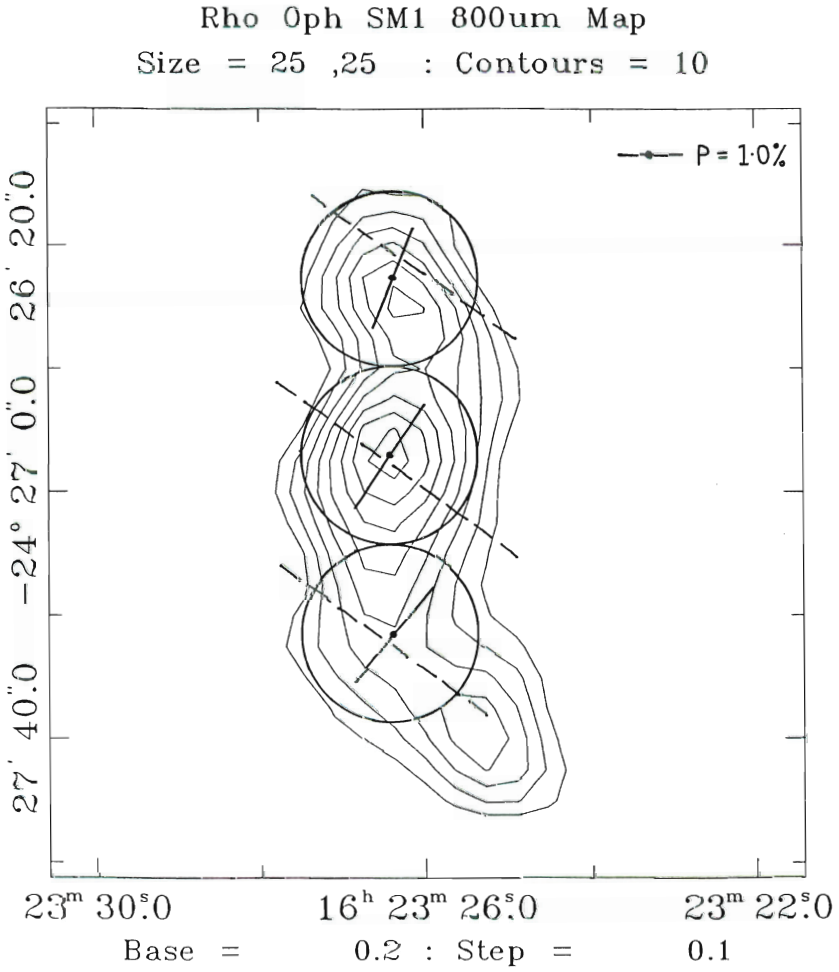

Figure 2. As in Figure 1, but for Rho Oph SM1.

Points of Contact

Joint Astronomy Centre
660 N. A'Ohoku Place
University Park
Hilo
Hawaii 96720
USA

JAC
Phone: 1-808-961 3756
1-808-935 4332 (answerphone)
Fax: 1-808-961 6516
e-mail: PSS: 315280809053
STARLINK: JACH
Internet: JACH.HAWAII.EDU
(from Janet
CBS%NSFNET-RELAY::EDU.HAWAII.JACH)

Mauna Kea
JAC Offices at Hale Pohaku 1-808-935 9911
JCMT Carousel: 1-808-935 0852
UKIRT dome: 1-808-961 6091
Fax in JCMT carousel: 1-808-935 5493

User manuals

Copies may be obtained by contacting:
Henry Matthews at JAC (JCMT)
Dorothy Skedd at ROE (UKIRT and JCMT)

The Newsletter is distributed in Canada by the HIA, Ottawa. Readers in Canada wishing to be placed on the mailing list should contact:

Dr John McLeod
Herzberg Institute of Astrophysics
100 Sussex Drive
Ottawa
Ontario K1A 0R6
Canada

Newsletter Editors:

ROE: Eve Thomson 031 668 8350
COS on REVAD
Mark Casali 031 668 8315
Graeme Watt 031 668 8310
JAC: Colin Aspin (CAA)

Please send material for the next edition of this Newsletter to an Editor by **December 15** - earlier if possible, please.

Royal Observatory Edinburgh
Blackford Hill
Edinburgh EH9 3HJ
UK

Telephone:
From outside UK, omit 0 & prefix by 44

Switchboard: 031 668 8100
JCMT & UKIRT Sections:
Dorothy Skedd 031 668 8306
Fax: 031 668 8264

e-mail:
Starlink: REVAD::UKIRT
or REVAD::JCMT
SPAN: 19898::UKIRT or 19898::JCMT
INTERNET: JCMT@UK.AC.ROE.STAR
or UKIRT@UK.AC.ROE.STAR

On-line Documentation
Captive accounts available on ROE Starlink cluster:
JCMT RESTAR::JCMTINFORM
UKIRT RESTAR::UKIRTINFORM
These are not currently directly available via Internet, but can be accessed as described on page 17.

Bulletin Boards and Vaxnotes conferences, available for your contributions and for information, are accessible to SPAN and STARLINK only, viz.

19898::JCMT, 19898::UKIRT and
19898::REMOBS (for remote observing).

The UKIRT Vaxnotes conference includes various subheadings including CGS4.

Service Observing

Applications should be sent by e-mail to the following:

for JCMT:
Canadian: JCMTSERV@HIARAS.HIA.NRC.CA
Dutch: ISRAEL@HLERUL51
UK: REVAD::JCMTSERV

for UKIRT:
REVAD::UKIRTSERV or
UKIRTSERV @ UK.AC.ROE.STAR

ISSN 0963-2700